Tutor/s

Dr. Rodrigo Soto López
Department of Chemical Engineering/ Analytical Chemistry

Dr. Javier Tejero Salvador
Department of Chemical Engineering/ Analytical Chemistry

Màster en Enginyeria Química

Treball Final de Màster

Kinetics of the isosorbide production from sorbitol using water as solvent and the ion-exchange resin CT-482 as catalyst.

Cinética de la producción de isosorbida a partir de sorbitol utilizando agua como disolvente y la resina de intercambio iónico CT-482 como catalizador.

María Padilla Ortín

June 2022

UNIVERSITAT DE BARCELONA

Dos campus d'excel·lència internacional
B:KC Barcelona Knowledge Campus
HUBC Health Universitat de Barcelona Campus

Report

CONTENS

1. SUMMARY

The chemical industry is subject to various trends and requirements. On the one hand, products must be safe for society. On the other hand, they can replace raw materials from oil or coal, reducing the environmental impact of the processes and reducing energy consumption. The use of bisphenol A has been banned because of the endocrine problems it causes in the population. Bisphenol A is a monomer used to produce polymers that coat the inner surface of tin cans, or was present in the heat-sensitive paper on which supermarket tickets are printed, for example.

To replace bisphenol A, the use of isosorbide, a monomer that can polymerize to give polymers of equivalent function to bisphenol A derivatives, has recently been proposed. Isosorbide can be obtained by a process that uses fructose or another sugar as a feedstock and can be produced from biomass after hydrolysis of wood or agricultural residues. Fructose is converted to isosorbide in two stages. In the first, fructose is converted to sorbitol by hydrogenation, and in the second, sorbitol, in the presence of an acid catalyst, forms isosorbide.

The aim of the present work was to begin the study of the second reaction, verifying that the reaction is possible using acid ion-exchange resins as catalysts and with special emphasis on obtaining kinetic data. These catalysts are suitable to work at moderate temperatures (below 130 ºC) and, therefore, in interesting conditions for energy saving. A reaction device was used that allowed working with sorbitol in aqueous solution. The working conditions that allow to operate selectively towards the isosorbide avoiding the effects of internal and external matter transfer were determined, using a catalyst previously selected by screening. All this, obtaining a good reaction rate. Finally, the kinetic model that best fitted the experimental results was determined.

Keywords: Sorbitol; isosorbide; bisphenol A; acid ion-exchange resins; liquid-phase reaction; kinetic modeling.

2. INTRODUCTION

Currently, the chemical industry bases its production on the use of fossil fuels as raw materials. Fossil fuels are hydrocarbons formed from fossilized organic residues. This transformation takes millions of years and is made possible by the high pressures and temperatures exerted by the sediments accumulated above. They are considered non-renewable energy sources and can be found in the following three physical states: in gas form (natural gas), in liquid form (crude oil or derivatives) and in solid form (coal).[1] During the 18th century, these compounds began to be commercialized as an energy source and, soon after, the potential of fossil derivatives was discovered. This generated an increase in demand both for energy and for the formation of products with diverse and excellent properties. From then until now, commercialization has become globalized.[2] This exponential increase in consumption and the difficulty of generating it in the medium or short term has led to the need for substitute materials.

In addition, the consumption of fossil fuels has been found to be dangerous to the environment. This is because they generate greenhouse gases (GHG), which is one of the main causes of global warming. Among the best known GHGs is the release of carbon dioxide (CO_2) after the combustion of petroleum products.[3] In order to counteract the global warming, severe measures have been considered for a progressive reduction of GHG emissions.[4] Another drawback derived from petroleum-derived compounds are the hazards for human, animal and plant health. For instance, Bisphenol A, a monomer with high stability and structural rigidity, has been found to be an endocrine disruptor that has serious effects on human health as well as inhibiting plant growth and development.[5] Polymers formed from this compound, currently banned, have excellent thermal and mechanical properties, and have been widely used in the plastics industry.[6]

In recent years, the industry opted for alternative compounds as substitutes for current petrochemical products [4] focusing on sustainable and renewable resources that are economically viable. These compounds are known as green chemicals and among the best known are those derived from non-edible biomass.[7] Biomass is a source of carbon from animal or plant organic matter that can be used as a raw material for energy production. It is a renewable energy source because the emission of CO_2 released during biomass combustion is equivalent to that consumed by plants during photosynthesis.[8]

The use of forestry and agricultural residues as a resource is of particular interest because they are widespread and easy to regenerate from biomass, but without interfering with the raw material used in the agricultural industry. These residues are known as non-edible biomass and are composed of 80% lignocellulose.[6] This amount of available raw material is sufficient to meet the high demand for fossil fuel substitutes and derivatives.

Lignocellulose is an organic substance present in plant cell walls and is composed of cellulose (40 – 50%), hemicellulose (25 – 35%) and lignin (15 – 20%). Cellulose is a polymer composed of linear chains of β-glucose molecules. Hemicellulose is a polysaccharide composed of two types of sugar monomer; pentose and hexose. Lignin is an aromatic compound formed by phenyl-propane units that provide structural rigidity to plants.[9] By means of a hydrolysis process in an acid medium, cellulose and hemicellulose can be transformed into C5 and C6 sugar monomers (i.e. glucose, fructose, xylose, arabinose),[10] which in turn can be further transformed into highly valuable platform chemicals.[11]

The U.S. Department of Energy published a report in 2004 with the main platform chemicals from biomass.[12] Among them is sorbitol, a compound that could be used to obtain various high value-added substances. One of the possible synthesis routes would be the double dehydration of sorbitol to obtain isosorbide. Other compounds with high potential from sugars are levulinic acid and furanic derivatives, such as 5-hydroxymethylfurfural and furfural.[13]

2.1. SORBITOL

Sorbitol (Figure 1, $C_6H_{14}O_6$), also known as glucitol, is a polyhydric alcohol produced by the chemical transformation of sugars derived from lignocellulose. It is usually marketed as a white crystalline powder and has a sweetness of approximately 60% sucrose.[14]

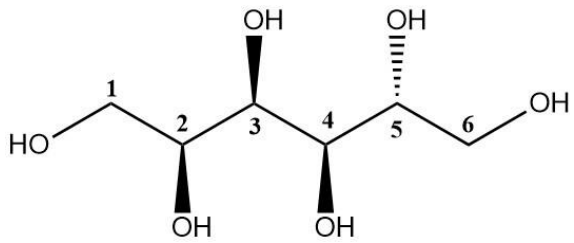

FIGURE 1.Chemical structure of sorbitol.

At the industrial level, sorbitol is widely used in the food sector as a sweetener additive. It is also used in the cosmetics and pharmaceutical industry as an anti-drying agent and preservative.

In addition, it is of particular interest to the chemical industry as a raw material to form a wide range of high value-added products.[15]

2.2. ISOSORBIDE

Isosorbide (Figure 2, $C_6H_{10}O_4$) is a bio-based chemical compound with the potential to be used in various applications bio-substitute for petroleum-derived compounds such as bisphenol A and other polymers.[16] This is due to its low toxicity, acceptable stability and functional versatility.[6] Isosorbide is composed of two fused tetrahydrofuran rings and two hydroxyl groups in endo-exo configuration. Due to its structure, the molecule presents two isomers depending on the configuration of the hydroxyl groups: isomannide when the configuration is endo-endo and isoidine when it is exo-exo. Consequently, the three molecules have different reactivities and physicochemical properties.[17]

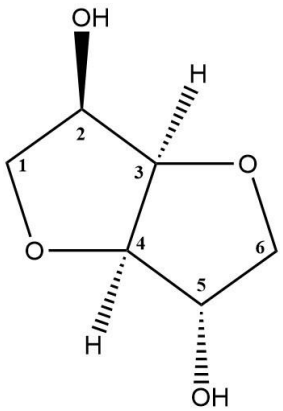

FIGURE 2. Chemical structure of isosorbide.

At industrial scale, isosorbide is synthesized by dehydrating sorbitol by homogeneous catalysis using mineral acids, such as sulfuric acid.[18] This presents a number of disadvantages like: acid corrosion derived problems and the need for separating the product from the catalyst. Noteworthy, current isosorbide production yields are lower than industry standards. This is why heterogeneous catalysts, e. g. by ion exchange resins, is envisaged as a plausible solution to overcome the mentioned limitations.

Within the exposed framework, this work provides a kinetic study on the isosorbide synthesis from sorbitol over a potentially applicable ion exchange resins, CT-482, selected from a previous screening study.[19]

2.3. CHEMICAL REACTION

The reaction system studied is the double dehydration of D-sorbitol to obtain isosorbide. It consists of 2 dehydration reactions in series, Figure 3. In the former, sorbitol is dehydrated to 1,4-sorbitan and, to a lesser degree, 3,6-sorbitan. In the layer, isosorbide is obtained through dehydration of 1,4-sorbitan and 3,6-sorbitan.[20] The parallel formation of side products is a drawback to be consider limiting sorbitol yields to isosorbide.

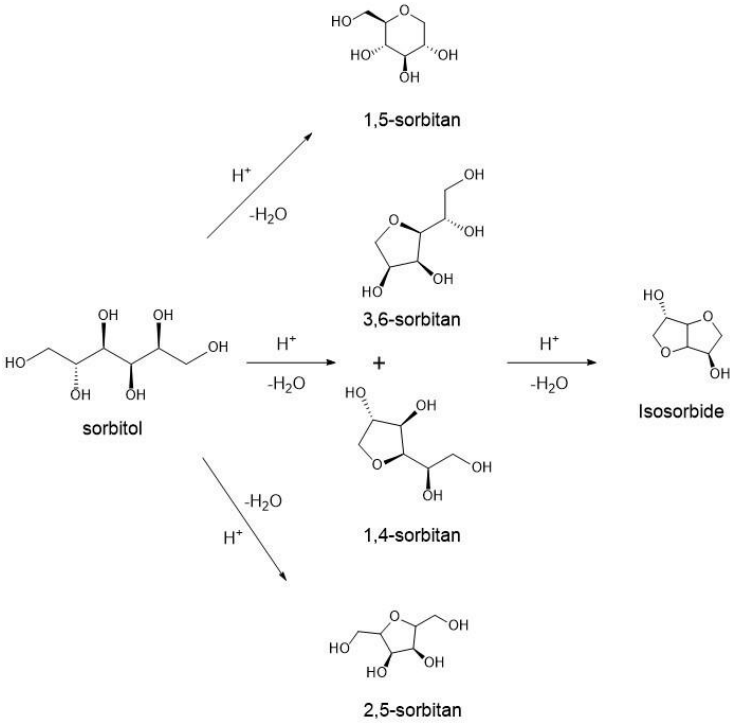

FIGURE 3. Double dehydration of sorbitol to isosorbide.

The main byproducts generated are: 1,5-sorbitan and 2,5-sorbitan. However, other the isomers involved in the reaction can also yield secondary products by molecular degradation. The result of this transformation is a variety of compounds of polymeric structure and insoluble character known as humins. The formation of these products prevents good isosorbide yields from being obtained.[21]

As discussed above, the use of solid heterogeneous catalysts is a good alternative to homogeneous catalysis. In the literature, previous studies investigated the use of different solid catalysts. Table 1 gathers the main result obtained in terms of reactants conversion and selectivity to target product along with the experimental conditions explored.

TABLE 1. Summary of experiments using heterogeneous catalysts. [19]

Catalyst types	Catalyst	Catalyst load	Solvent	T [ºC]	t [h]	X_{SOH}[a] [%]	Selectivity [%]		
							IB[b]	1,4ST[c]	Others
Metal phosphate [22,23]	SnPO	0.5 g	Water (SOH 10wt%)	300	2	72	65	34	1
	ZrPO	0.5 g	Water (SOH 10wt%)	300	2	56	52	26	22
	TiPO	0.5 g	Water (SOH 10wt%)	300	2	97	46	3	51
	BP	1 wt%	Water (SOH 70wt%)	250	2	100	70	6	-
Zeolites [24]	Beta(75)	SOH/Al=50	Water (SOH 9wt%)	200	2	87	33	43	24
	Beta(150)	SOH/Al=50	Water (SOH 9wt%)	200	2	73	22	56	22
	Mordenite(110)	SOH/Al=50	Water (SOH 9wt%)	200	2	60	20	55	25
Acid resins [25]	P-CT275	5 wt%	Free	140	1,5	96	40	-	-
	P-CT269	5 wt%	Free	140	1,5	93	33	-	-
	Amberlyst 70	5 wt%	Free	140	1,5	92	31	-	-
	Amberlyst 35	5 wt%	Free	140	1,5	91	31	-	-

(a) sorbitol conversion
(b) Isosorbide
(c) 1,4-sorbitan

From this table it can be concluded that higher sorbitol conversions are obtained with ion-exchange resins, although the selectivities are still low. They also allow working at lower temperatures. For this reason, the study will focus on the use of ion-exchange resins as a catalyst for the reaction.

2.4. ACID ION-EXCHANGE RESINS

A catalyst is a substance that increases the rate at which a chemical reaction approaches equilibrium without permanently intervening in the reaction. Depending on the nature of the catalyst, catalysis can be classified into the following three types: homogeneous, heterogeneous and enzymatic. Homogeneous catalysis is considered when the catalyst and reactants are in the same phase and heterogeneous when they are in different phases. The term of enzymatic catalysis is coined when the catalyst is an enzyme. Approximately 80% of industrial catalytic processes are heterogeneous and, of these, 90% use solid catalysts.[26]

When solid catalysts are used, it is necessary that at least one of the reagents can adsorb on the surface of the solid. In turn, the catalyst must have a large adsorption surface to facilitate the interaction between the reagent and the solid, as is often the case with porous solids. Another factor to take into account is the performance of the catalyst in terms of its activity. This is typically related to structural properties, e.g., pores size and volume. In addition, it is important to know the chemical composition of the catalyst since the interaction with the reagent is of chemical nature and this is related to the type of functional groups that are the actual active sites.

At industrial level, the interest in a given solid catalyst is evaluated in terms of selectivity, lifespan and activity. Activity refers to the catalyst's ability to transform reactants into products. Selectivity corresponds to the capacity to produce the desired compound with respect to the total number of products obtained. And the lifespan consists of the period of time in which the activity and/or selectivity satisfy the needs of the process, i. e. without signs of deactivation.

Solid catalysts generally consist of a support and an active phase. The support is a material with a large surface area that contains the active component stabilized. The active phase or component is responsible for increasing the reaction rate. Sometimes catalysts can also have promoters to enhance the activity of the catalyst. The elementary chemical stages of a solid catalytic reaction taking place in the active sites are: adsorption of reactants, chemical reaction and desorption of the product.

Ion exchange resins are organic polymers with the capacity to exchange ions with the medium in which they are working. Their structure consists of a polymeric matrix of hydrocarbon chains with functional groups anchored to it. The cross-linking agent gives the matrix a stable three-

dimensional hydrophobic structure with a defined pore structure.[27] These resins are usually marketed as spherical particles between 0.3 and 1.2 mm in diameter.[28] There are two main types of resins due to the degree of cross-linking they present: gel-type and macroreticular resins. Low cross-linked resins have a microporous structure (gel-type) and high cross-linked resins have a macroporous structure (macroreticular). The degree of cross-linking affects the level of porosity, which in turn influences some of their properties.[29] They are also differentiated according to pore diameter: ultra-micropone type for sizes smaller than 0.7 nm, micropones for sizes between 0.7 and 2 nm, mesopones for sizes between 2 and 50 nm and macropones for sizes larger than 50 nm.[30] As a result, resins can have different applications depending on their structure. The most used ion-exchange resins are those with a styrene-divinylbenzene support (PS-DVB). These can be obtained through a process of copolymerization of styrene and divinylbenzene (cross-linking agent).[31]

After obtaining the support structure, the functional groups (acid, basic, metallic, etc.) are added to the resin to build a catalyst with the required properties for a reaction. In the case of acid sites, a sulfonation process is carried out by means of a bath with concentrated sulfuric acid. Depending on the degree of sulfonation of the resin, three different groups are distinguished: over-sulfonation (OS), conventional sulfonation (CS) and surface sulfonation (SS), in order from the most to the least sulfonated. The parameters that determine the use of a particular resin are: degree of cross-linking, swelling, stability, particle diameter, density, water affinity, acid capacity and acid strength. These parameters are usually obtained by dry analytical processes, to avoid the change of structure upon swelling due to contact with a solvent. However, it is also important to determine these parameters when the particles are swollen, for example, by ISEC (Inverse Size Exclusion Chromatography).[32]

The use of ion exchange resins is subject to chemical, mechanical and thermal stability. Chemical stability is given by the resistance of the resin structure not to degrade when working in oxidizing conditions. Mechanical stability is defined as the resistance of the particle to breakage and compression. Thermal stability corresponds to the ability of the resin to resist high temperatures. Each resin has a maximum operating temperature above which irreversible changes occur in its structure and, consequently, a decrease in catalytic activity.[27] Knowledge of the above parameters is useful for understanding the catalytic behavior of a resin in the reaction environment.[29] Therefore, studies have been carried out to determine which types of acid ion-exchange resins are best for the production of isosorbide from sorbitol dehydration. The resin that

obtained the best results was the thermostable CT-482.[19] Basic information on this resin can be found in Table 2.

TABLE 2. Properties of ion exchanger CT-482. [19]

Catalyst	Type	Acid capacity [mmol H^+/g]	DVB% [%]	Water retention [%]	T_{max} [ºC]	dp [mm]	d_{pore} [nm]	S_g [m^2/g]	V_{pore} [cm^3/g]	V_{sp} [cm^3/g]	θ [%]
CT-482	macro	4,25	LOW	48-58	190	0.81[a]	26.7[a]	8.7[a]	0.06[a]	-	8.2[a]
						-	19.6[b]	214.0[b]	1.05[b]	1.081[b]	65.7[b]

[a] Dry state: measured by BET technique
[b] Swollen in water: measured by ISEC technique.

2.5. PHYSICOCHEMICAL STEPS ON HETEROGENEOUS CATALYSIS

When a reaction system is catalyzed by a solid, the reaction rate is characterized by the resistances found from the time the reactant travels from the fluid and interacts with the particle until the product is obtained and released from the catalyst. These resistances have been classified into 7 elementary stages that make up the catalytic process:

1) *External mass transfer of reactants*: It consists of the diffusion of the reactants from within the fluid phase to the surface of the film enveloping the catalyst.
2) *Internal mass transfer or diffusion of reactants*: where intraparticle diffusion of reactants into the catalyst pores from the outside to the active sites takes place.
3) *Adsorption of reactants*: on active sites.
4) *Chemical reaction*: surface reaction between adsorbed reactants to form adsorbed products.
5) *Desorption of products*: of active sites.
6) *Internal mass transfer (or diffusion) of the products*: where intraparticle diffusion of products occurs through the catalyst pores from the active sites to the outside.
7) *External mass transfer of products*: corresponds to the diffusion of products through the film enveloping the particle into the fluid phase.

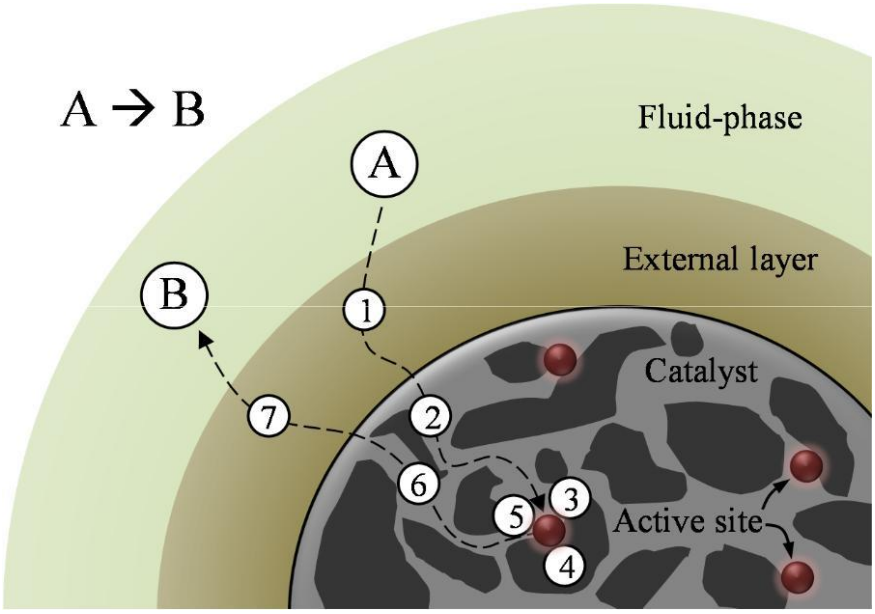

FIGURE 4. Steps of the catalytic process of reaction A ↔ B in porous solid.[32]

In Figure 4, points 1, 2, 6 and 7 are of physical related to mass transfer while points 3, 4, and 5 are chemical steps. In order to obtain a kinetic model of a chemical reaction, it is considered that the stages occur in series-parallel except for the internal mass transfer, which occur in series. In brief, there are three different kinetic controlling regimes: external mass transfer (1 and 7), internal mass transfer (2 and 6) and chemical reaction (3, 4 and 5).[26]

The overall reaction rate is marked by the limiting step corresponding to the step that has a significantly lower rate than the rest. Both external mass transfer (EMT) and internal mass transfer (IMT) can influence the reaction rate. EMT occurs when concentration and temperature profiles occur in the external film around the catalyst and reactants concentration at the external catalyst surface is nile, while IMT refers to concentration and temperature profiles generated between inside the catalyst particle. Accordingly, the smaller the particle size the higher the internal diffusivity and the higher the stirring speed the lower the effect by EMT.[27] For determining that the limiting stage of the reaction is the chemical reaction at the pores surface, it is necessary to perform experiments to determine the conditions at which the agitation in the reactor and the particle size are not leading to a physical control of the kinetics. Under such conditions, the reaction rate is governed by the chemical stages and the kinetic expressions of the intrinsic reaction rate.[32]

2.6. MECHANISTIC MODELS OF SURFACE REACTION IN HETEROGENEOUS CATALYSIS

The classical models of heterogeneous are based on the Langmuir-Hinshelwood-Hougen-Watson (LHHW) and Eley-Rideal (ER) formalisms. In the first model, all reactants are considered to be adsorbed on the active sites and react with each other. Conversely, in the second model not all reactants are adsorbed on the catalytic surface and the reaction occurs between adsorbed and non-adsorbed reactant molecules. In both cases the resulting product is adsorbed.[33] Typically, the equations representing this mechanisms comprise the kinetic term, the driving force, the adsorption group and the number of active centers involved in the reaction.[27]

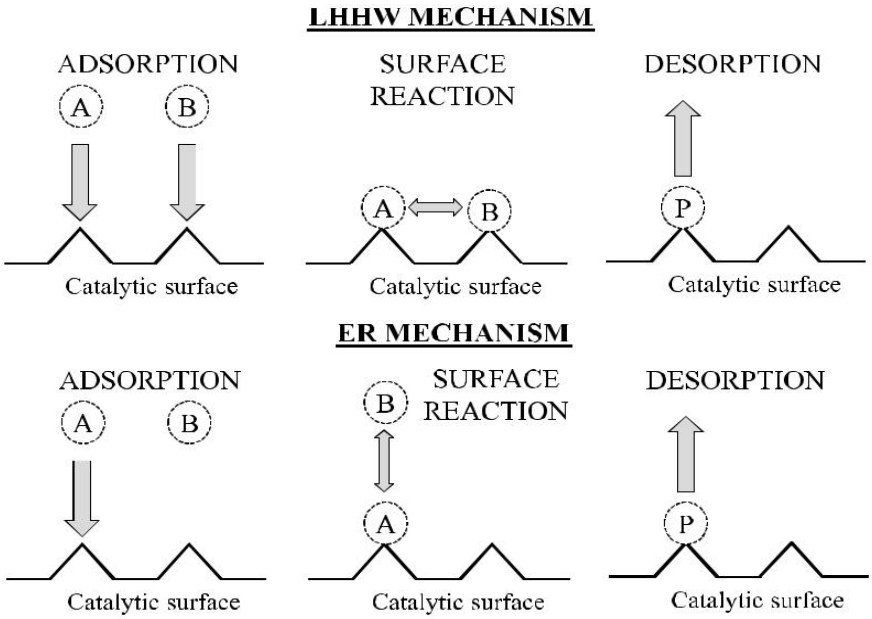

FIGURE 5. Schematic representation of LHHM and ER methods for A + B ↔ P reaction. [27]

Interestingly, the information that can be found in the open literature about the kinetics of the isosorbide production from sorbitol dehydration over solid acid catalysts is very scarce. Only a very recent study evaluated the thermodynamics and kinetics of this reaction system catalyzed by $NbOPO_4$. By thermodynamic analysis they concluded the double dehydration is an endothermic process in which the first stage has an irreversible behavior while the second stage is reversible. Therefore, working at high temperatures favors the positive shift of the equilibrium towards the second step of dehydration. They proposed a pseudo-homogeneous first order reaction model

which satisfactory fits to experimental data at temperatures ranging 493.15 – 523.15 K. However, at high temperatures the side reactions are favored over because of their higher activation energy. In order to maximize the isosorbide yield, the authors proposed an operating system consisting of two stages at different working temperatures.[34] From such study, it can be concluded that there is a need for finding a potential catalyst for this reaction system able to operate at lower temperatures. This is precisely one of the motivations of the present project; to assess whether an ion-exchange resin can provide similar activity and selectivity at lower reaction temperatures.

3. OBJECTIVES

The main objective of the present work is to perform a kinetic study on the synthesis of isosorbide from sorbitol using water as solvent over the thermostable acidic ion-exchange resin CT-482. To achieve it, the following subobjectives are set:

- To condition the experimental setup where the experimental runs will be conducted and to develop the analytical methods necessary for tracking the product distribution over time.
- To perform a study of the mass transfers (internal and external) influences on reaction rates aimed at determining the conditions at which they can be considered negligible, so the surface reaction is the controlling step.
- To study the effect of the catalyst load on reaction rates in order to set the catalyst mass used in the experiments.
- To execute a rigorous experimental design for obtaining reliable kinetic data for the involved species in the studied reaction system. The experiments will be carried out at different temperatures and different initial composition of the reaction mixture in order to obtain a wide variation of the expected non-linear profiles that can represent faithfully the involved kinetics.
- To assess the effect of experimental conditions on reactants conversion, selectivity and yield towards target product, in order to find out the conditions promoting the formation of isosorbide.
- To estimate the reaction rates of consumption and formation during the runs for the involved species.
- To propose a kinetic model based on the LHHW and ER formalisms able to predict reliably the kinetics of the studied system, contributing thereby to improve our knowledge on the reaction mechanisms through which the involved reactions occur.
- Noteworthy, the assessment of the involved parameters to estimate in each model, e.g., kinetic constants, activation energies and adsorption equilibrium constants, is also a fundamental part of this work.

4. EXPERIMENTAL SECTION

4.1. CHEMICALS & CATALYST

The synthesis of isosorbide was performed using sorbitol as reactant (Alfa Aesar, 98% purity) and using deionized water (Mili-Q, Milipore) as solvent. In addition, the following analytical standards were used for the calibration of the analysis system: isosorbide (Alfa Aesar, 98% purity) and 1,4-sorbitan (Sigma-Aldrich, >99% purity). Although 2,5-sorbitan was detected as by-product in all the runs, its calibration was performed the 1,4-sorbitan responses since its congener was not commercially available. Some physicochemical properties of the main chemical species involved are gathered in Table 3.

TABLE 3. Main properties of the reactants and products.

PROPERTIES	Sorbitol[b]	1,4-Sorbitan[c]	Isosorbide[d]	2,5-Sorbitan[e]
Formula	$C_6H_{14}O_6$	$C_6H_{12}O_5$	$C_6H_{10}O_4$	$C_6H_{12}O_5$
CAS number	50-70-4	27299-12-3	652-67-5	27826-73-9
Molecular Weight [g/mol]	182.17	164.16	146.14	164.16
Density [g/cm^3] [a]	1.49	1.57	1.5	1.48
Meiling point, T_m [ºC]	98-100	112-113	60-63	56-57
Boiling point, T_b [ºC]	295	443	175	416.2

[a] at T=25ºC.
[b] Value obtained from Alfa Aesar.
[c] Value obtained from Sigma-Aldrich and Chemical book.
[d] Value obtained from Sigma-Aldrich, Chemical book and ChemSrc.
[e] Value obtained from Chemical book and Ningbo Inno Pharmchem.

As aforementioned, Purolite CT-482 was used as the catalyst for the present kinetic study based on a preliminary screening study. It consists of a commercially available acidic macroreticular ion-exchange resin with thermostable features, with the physicochemical and morphological properties summarized in Table 2.

4.2. EXPERIMENTAL SETUP

The experimental setup consists of a stainless steel batch reactor (316 SS) of 100 mL useful volume (Autoclave Engineers, Inc. Serial No. 98250114-1) equipped with an overhead stirrer, an electric furnace for controlling the heating and a catalyst injector. The agitation was provided by a four-bladed 45° inclined impeller mounted on a rotor (Magnedrive II Series 0.75-01) connected to a frequency converter (T-VERTER N2 SERIES) to regulate the agitation speed. A baffle is located next to the impeller to ensure homogenization of the mixture. The heating system consists of an electric furnace connected to a PID temperature control system through two thermocouples that measure the temperature inside the reactor and on the outside wall. After reaching the set point, its value is kept constant with a ± 0.1 ºC error. The reaction temperature was varied between 150–190 °C and the pressure was kept constant at 30 bar using N_2 (99.9995 %GC, Abelló Linde). This pressure was set to ensure the liquid-phase of the reactants mixture, i.e. by exceeding its vapour-pressure at all temperatures explored, and to impel the samples taken at any instant from the reactor towards the implemented sampling port. It also consists of a cylindrical injector (316 SS) to introduce the catalyst into the reaction system. In addition, it contains a relief valve, a pressure gauge, a filter and a rupture disk. The latter allows instantaneous pressure release when the working pressure exceeds the maximum pressure (50.1 – 54.8 bar). A schematic representation of the experimental device used is illustrated in Figure 6.

For the analysis of the samples, a High-Performance Liquid Chromatograph (HPLC, Agilent Infinity Series II) equipped with a refraction index detector (RID) was used. The HPLC column used was a 250 x 4.6 mm Hi-Plex Ca (Agilent Technologies Ltd.) using Millipore grade water as mobile phase. The main parameters of the chromatographic method developed are summarized in Table 4.

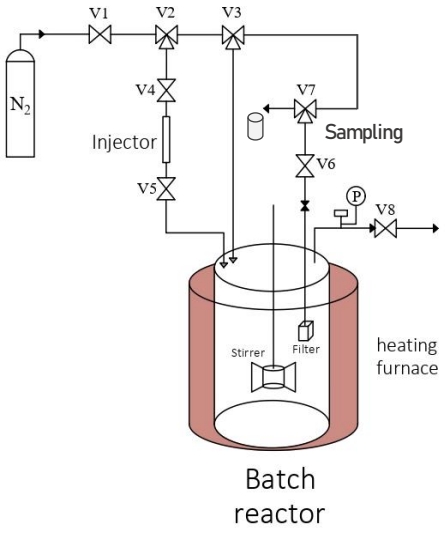

FIGURE 6. Scheme of the experimental Set up.

TABLE 4. HPLC method

Quat. Pump		
	Flow:	0.300 mL/min
	Solvents:	100% Millipore water
	Stoptime:	17.00 min
	Posttime:	Off
Pressure Limits	Min:	0.0 bar
	Max:	400.0 bar
Advanced	Minimum Stroke:	Automatic
	Compressibity:	$50*10^{-6}$ /bar
	Maximum Flow Gradient:	100.000 mL/min^2
	Primary Channel:	Automatic
Column Comp.		
	Temperature Left:	80.0 ºC
	Temperature Right:	Combined
	Stoptime:	As Pump/Injector
	Post Pump:	Off
Advanced	Enable Analysis Left:	When temperature is within ± 0.8 ºC
	Enable Analysis Right:	When temperature is within ± 0.8 ºC
RID		
	Optical Unit Temperature:	35.00 ºC
	Signal:	Acquire
	Peakwidth:	> 0.2 min (4 s response time) (2.31 Hz)
	Stoptime:	As Pump/Injector
	Post Pump:	Off
Advanced	Analog Output	
	Zero Offset:	5 %
	Attenuation:	500000 nRIU
	Signal Polarity:	Positive (+)
	Automatic Zero Before Analysis:	On
	Automatic Recycling After Analysis:	Off

4.3. CATALYST CONDITIONING BEFORE THE ACTIVITY RUNS

The catalyst preparation consisted of three phases: drying at atmospheric temperature, particle size reduction/separation, and oven drying. For drying at room temperature, the catalyst is placed in a paper container for 24 to 48 hours. Afterwards, the catalyst was crushed in a mill and separated using metallic sieving plate in the following particle sizes: larger than 0.4 mm, 0.4 - 0.25 mm, 0.25 - 0.16 mm, 0.16 - 0.08 mm and smaller than 0.08 mm. Finally, the catalyst of the desired size was dried in an oven at 110°C for 24 hours before the catalytic activity runs.

4.4. EXPERIMENTAL AND ANALYTICAL PROCEDURES

The first step is to prepare the reaction mixture; sorbitol diluted in water. For this, water and sorbitol are weighed separately and added to the reactor. Next, the system was closed with the three safety screws and a leak test was performed to verify that there were no leaks. The electrical jacket was placed around the reactor and the stirring and heating systems were turned on. Once the reference temperature was reached, the dry catalyst previously placed in the injector was injected. For a correct injection, there had to be a pressure difference of 20 bar. This had to be done as quickly as possible due to the hygroscopic behavior of the catalyst. The injection process was repeated about 5 times to ensure that it was completely injected.

The first sample was then drawn at the initial or zero time (t=0). Thereafter, samples were taken every half hour until 2.5 hours of reaction, then every hour until the experimental time of 6.5 hours was reached. These were collected in a vial with a leaky lid. The mixture retained in the circuit was recirculated to the reactor. After allowing the vial to cool, 0.5 mL of sample were extracted and diluted 1:2 with Millipore water in a 1.5 mL vial. Once the samples were diluted, they were analyzed in the high-performance liquid chromatograph (HPLC) under the operating conditions shown in Table 4. If the RID detector was saturated by the analyzed sample, it was further diluted to 1:4 with Millipore water.

4.5. EXPERIMENTAL CONDITIONS

The main objective of the project was to perform the kinetics of the isosorbide production from sorbitol reaction system. Accordingly, it was necessary to determine the experimental conditions at which the internal and external diffusion effects could be considered negligible compared to the surface reaction, this being the limiting stage. To this end, it was proposed to divide the experimental phase into 4 stages. The first two stages would be the study of the effect of internal transfer of matter (ITM) and external transfer of matter (ETM). For ITM, four experiments were carried out at different particle diameters and the effect on the reaction rate was analyzed. Then, four more experiments were carried out for ETM. The experiments were carried out at different stirring speeds with the particle size chosen from the first study. Once these two criteria were evaluated, the analysis of the effect of catalytic loading on the reaction rate was continued by 3 additional experiments. Finally, the last block of the experimental design, the kinetic study, was carried out. It consisted of 15 experiments at different initial sorbitol concentrations and temperatures under the previously determined operating conditions.

TABLE 5. Experimental conditions.

STAGE	**Temperature** (ºC)	**Agitation** (rpm)	$\mathbf{m_{SOH}}$ (g)	$\mathbf{d_p}$ (mm)	$\mathbf{W_{cat}}$ (g)
ITM	190	750	4,5	<0,08 0,08-0,16 0,16-0,25 0,25-0,4 Commercial	0,75
ETM	190	250 500 750 1000	4,5	0,16-0,25	0,75
Catalyst Load	190	750	4,5	0,16-0,25	0,375 0,75 1,5
Kinetic study	150 160 170 180 190	750	2,25 4,5 9	0,16-0,25	0,75

4.6. GENERAL CALCULATIONS

The conversion (X_k), Eq. 3.6.1, corresponds to the amount of reactant consumed with respect to the initial amount of the same reactant. The selectivity (S_k^j), Eq. 3.6.2, is defined as the fraction between the moles of product or by-product formed versus the total moles of reactant consumed. And the yield (Y_k^j), Eq. 3.6.3, is obtained by multiplying the above two parameters.

$$X_k = \frac{mole\ of\ k\ reacted}{inicial\ mole\ of\ k} \qquad \textit{(Eq. 4.6.1)}$$

$$S_k^j = \frac{mole\ of\ j\ produced}{mole\ of\ k\ reacted} \qquad \textit{(Eq. 4.6.2)}$$

$$Y_k^j = X_k \cdot S_k^j \qquad \textit{(Eq. 4.6.3)}$$

where *k* corresponds to the reactants consumed and *j* to the products or by-products formed. Considering that there is only one reactant and the stoichiometry of the involved reactions, the moles of reactant consumed would be equal to the moles of products formed. Therefore, for the case studied, the following equations are derived:

$$X_{SOH}(t) = \frac{n_{SOH}^0 - n_{SOH}(t)}{n_{SOH}^0} \qquad \textit{(Eq. 4.6.4)}$$

$$S_j(t) = \frac{n_j(t)}{n_{IB}(t) + n_{1,4-ST}(t) + n_{2,5-ST}(t)} \qquad \textit{(Eq. 4.6.5)}$$

$$Y_j(t) = X_{SOH}(t) \cdot S_j(t) \qquad \textit{(Eq. 4.6.6)}$$

4.7. KINETIC MODELLING

As the experimental system works in discontinuous, the experimental rates of consumption or formation of the different species at any time can be estimated through the derivative of the corresponding mol evolution by, Eq. 4.7.1:

$$r_i = \frac{1}{W_{cat}} \cdot \left(\frac{dn_j}{dt}\right)_t \qquad \textit{(Eq. 4.7.1)}$$

Where r_i refers to the reaction rate of compound i at time t, n_j are the moles of compound i and W_{cat} is the dry mass of the catalyst used. The mole evolution curve of the reactant sorbitol was obtained by fitting an exponential type equation (Eq. 4.7.2) with two parameters to be adjusted, *a* and *b*. The target and secondary products were fitted with a function called Exponential Association (Eq. 4.7.3). This also had two parameters to fit (*a* and *b*). The two functions used are shown below, respectively:

$$n_j = a \cdot e^{-bt} \qquad \textit{(Eq. 4.7.2)}$$

$$n_j = a \cdot [1 - e^{-bt}] \qquad \textit{(Eq. 4.7.3)}$$

Once the experimental reaction rates have been estimated, a kinetic modelling was performed to assess the models that better fit the experimental data. For this purpose, the kinetic expressions were based on the following three hypotheses: there is a constant number of active sites on the surface of the solid particle, the proportions of the active sites are all equal and the reactivity of the active sites is only temperature dependent. The last two hypotheses do not coincide exactly with reality in the case of ion exchange resins. However, the expressions obtained using these considerations usually explain well the experimental variation in the catalytic reaction. The mechanistic models evaluated are based on the Langmuir-Hinshelwood-Hougen-Watson (LHHW) and Eley Rideal (ER) formalisms, having a general expression that can be summarized as:

$$r_i = \frac{\{Kinetic\ term\}_i \cdot \{Driving\ force\}_i}{\{Adsorption\ term\}^{n_i}} \qquad \textit{(Eq. 4.7.4)}$$

The general expression is composed of the kinetic term, the driving force, the adsorption term and an exponent n. The kinetic term is composed of the kinetic constant for reaction i. Sometimes, it can also include an adsorption equilibrium constant if the reaction mechanism requires it. For this case only the kinetic constant (k_i) was considered.

The driving force (Eq. 4.7.5) corresponds to the difference between the concentrations of reactants and products of the species involved in reaction i. This is defined according to the following expression where C_j would be the concentrations of the substances involved, ν_{ij} the stoichiometric coefficient of species j in reaction i and K_i is the equilibrium constant of reaction i.

$$\{Driving\ force\}_i = \left(\prod_{j=1}^{reactants} C_j^{\nu_{ij}} - \frac{\prod_{j=1}^{products} C_j^{\nu_{ij}}}{K_i} \right) \qquad \textit{(Eq. 4.7.5)}$$

The adsorption term (Eq. 4.7.6) represents the active centers occupied by the adsorbed species on the catalyst surface. Therefore, this term was assumed to be independent of the reaction; identical for all the reactions studied. K_j corresponds to the adsorption equilibrium constant of compound j in liquid phase, C_j would be the concentration of substance j and S would be the number of adsorbed species. The parameter α depends on whether the fraction of unoccupied active sites is significant or not, taking a value of 1 or 0 depending on that criterion.

$$\{Adsorption\ term\} = \alpha + \sum_{j=1}^{S} K_j \cdot C_j \qquad \textit{(Eq. 4.7.6)}$$

The exponential parameter of the adsorption term (n_i) can have values between 0 and infinity. For this study it was decided to analyze the values of 1, 2 and 3, since they are the most common values.

Both kinetic and equilibrium constants (Eq. 4.7.7) are dependent on the operating temperature. The adsorption equilibrium constant follows the van't Hoff function which depends on the adsorption entropy ($\Delta_{ads}S_j^0$) and the adsorption enthalpy ($\Delta_{ads}H_j^0$). From this, the parameters K_{1j} and K_{Tj} are extracted, which can be considered constant over the temperature range studied. The difference between the inverse of the operating temperature and the mean temperature ($\overline{T}$) is present to decrease the correlation between the parameters. The value of the average temperature used is 463.15 K.

$$K_j = e^{\left(\frac{\Delta_{ads}S_j^0}{R} - \frac{\Delta_{ads}H_j^0}{R}\left(\frac{1}{T}-\frac{1}{\overline{T}}\right)\right)} = e^{\left(K_{1,j}+K_{T,j}\cdot\left(\frac{1}{T}-\frac{1}{\overline{T}}\right)\right)} \qquad \textit{(Eq. 4.7.7)}$$

According to the Arrhenius law, the kinetic constants are also temperature dependent. Therefore, these constants also follow the above function from which the parameters k_{1j} and K_{Tj} need to be determined. The same is true for the equilibrium constant of the reaction.

The main objective is to estimate the parameters values in each model providing a good fit of all the reactions simultaneously. This requires minimizing the residual sum of squares between the experimental (r_i^{exp}) and calculated (r_i^{cal}) values of reaction rates, Eq. 4.7.8.

$$RSS_i = \sum_{i=1}^{S} \left(r_i^{exp} - r_i^{cal}\right)^2 \qquad \textit{(Eq. 4.7.8)}$$

Where RSS_i corresponds to the sum of residual squares for the evaluated velocities, r_i the reaction rate of species i and S the total number of species evaluated.

5. RESULTS

5.1. PRODUCT DISTRIBUTION OVER A TYPICAL RUN

The reaction system studied can be summarized in the following reaction scheme:

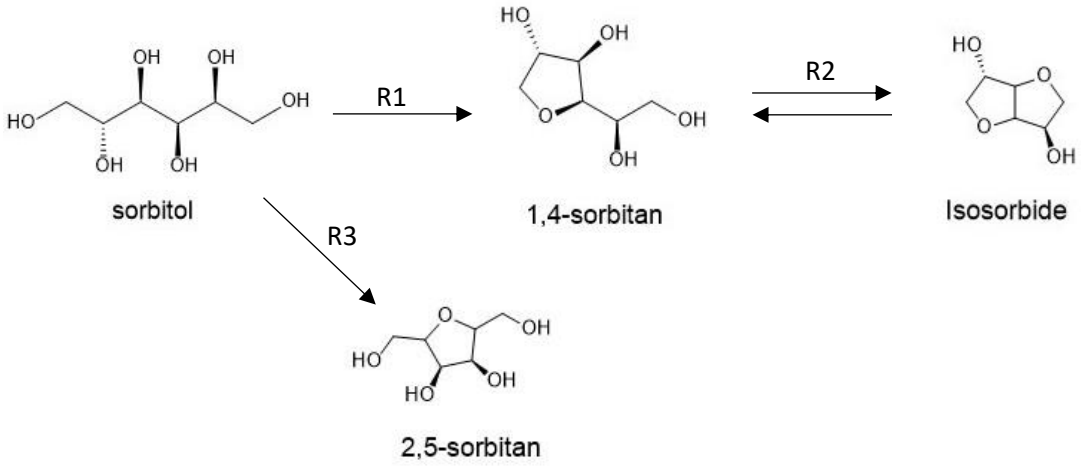

FIGURE 7. Scheme of the reaction.

The HPLC analysis enabled to obtain the mole evolution of each species using the analytical calibration. The main species found were: sorbitol (SOH), isosorbide (IB) and 1,4-sorbitan (1,4-ST). The fourth signal showed an increasing trend until it stabilized, which coincided with the almost total consumption of sorbitol. It was therefore concluded that the fourth substance present in the analysis corresponded to the secondary product. Different authors detected that the most common secondary sorbitan was 2,5-sorbitan (2,5-ST), so the signal was considered to correspond to this compound.[18,21] 2,5-sorbitan was not found commercially so it was decided to use the 1,4-sorbitan calibration for its quantification, because they are isomers. Figure 8 shows examples of the mole evolutions obtained at two opposite temperature conditions, the lowest (150 ºC) and the highest explored (190 ºC).

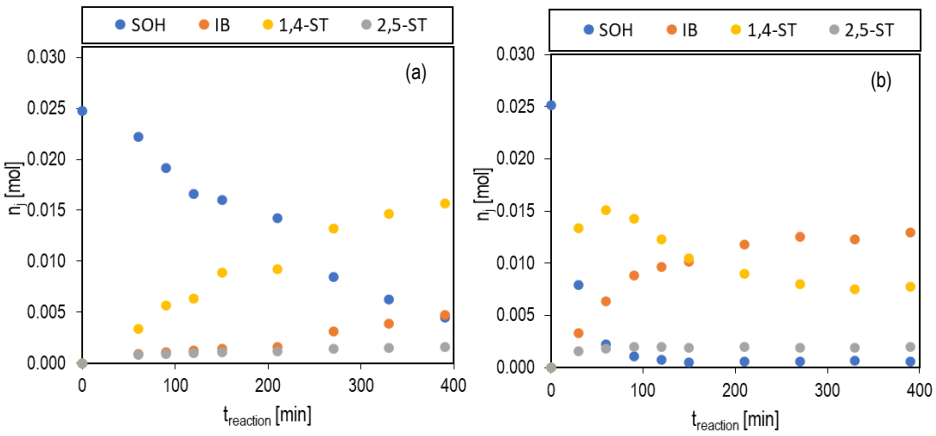

FIGURE 8. The variation of concentration for each species versus reaction time (a) 4.5 g SOH, 0.75 g CT-482, 750 rpm, T = 150 ºC and (b) 4.5 g SOH, 0.75 g CT-482, 750 rpm, T = 190 ºC.

The reaction mechanism of isosorbide synthesis from sorbitol is composed of two series reactions. In the first reaction the intermediate 1,4-sorbitan is formed which, in turn, is consumed in the second reaction yielding isosorbide. As mentioned above, a parallel reaction also occurs in the first stage, where 2,5-sorbitan is generated. Figure 7 shows the reaction system studied.

In Figure 8, it was observed how sorbitol goes from being consumed slowly over time to being practically exhausted after 2 hours at 190 ºC. This shows that the temperature increase accelerates the formation of 1,4-sorbitan and isosorbide. Due to the observed behavior, it was concluded that the reactions follow a series-parallel scheme, since the isosorbide starts to appear after a large part of the sorbitol is consumed but before the 1,4-sorbitan reaches its maximum. At a temperature of 190°C, the isosorbide curve was observed to increase until it stabilized. This fact was also reflected for 1,4-sorbitan, where it reached a maximum and then decreased until it stabilized. The behavior of both species showed that the second dehydration (R2) could present a reversible behavior. To confirm this possibility, the thermodynamic study of the reaction mechanism should be performed. Finally, it was observed that the formation of the secondary product did not vary much over the range of temperatures studied. This differs from that reported in the literature because they worked with lower temperatures than those used by other authors, e.g., ranges of 220 – 250 ºC.[34]

5.2. EFFECTS OF THE CATALYST LOAD, INTERNAL AND EXTERNAL MASS TRANSFERS

For the three studied blocks prior to the kinetic runs free of mass transfer, it was decided to work at 190 ºC because it is at the highest temperature where the effects of the catalyst load, the IMT and the EMT are more noticeable.

For the ITM study, the reaction rates were determined using different catalyst particle sizes. Theoretically, the smaller the particle size, the higher the internal diffusion of the species from the particle film to the interior of the pore. Figure 9 shows the variation of the initial reaction rate for the different compounds in relation to the reverse of the particle size analyzed.

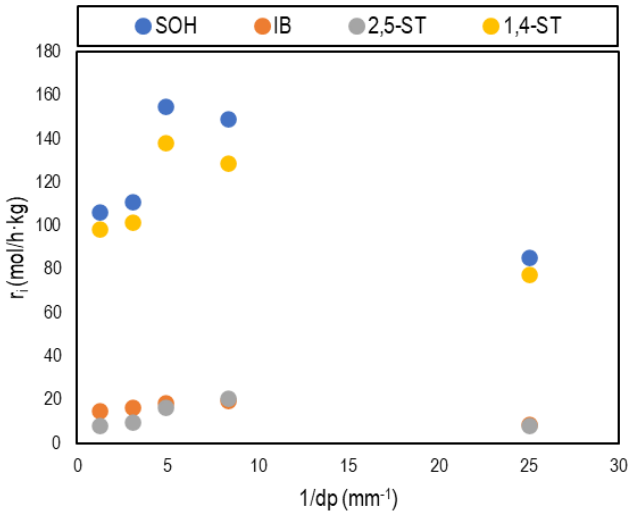

FIGURE 9. Effect of ITM on the initial reaction rate (0.75 g CT-482, 4.5 g SOH, 190 ºC and 750 rpm).

With the results shown in Figure 9 it was demonstrated that the smaller the size, the higher the reaction rate. In it, an increase in the reaction rate can be observed at smaller particle diameters. However, at very small sizes (d_p < 0.08 mm) such velocity decreased drastically. This was due to the flow problems caused by working with such small particle diameters. When working with particle sizes smaller than 0.08 mm, the particles resembled dust, creating some resistance to flow. This caused part of the catalyst not to be injected correctly into the reactor and, therefore, an unknown catalyst concentration. This fact discarded the use of this size for the kinetic study.

It was decided to use a particle diameter between 0.16 – 0.25 mm since the reaction rates were maximum for that size. Sizes between 0.25 – 0.4 mm were not used because the reaction rate value is lower than the other values. This is caused by an increase in the flow resistance of the compounds present in the reactions generating a decrease in the velocity. That is to say that at sizes larger than 0.25 mm the effect of TIM on the reaction rate can be considered significant.

For the ETM study, the reaction rates of each species involved were obtained at different agitation speeds. The theory indicates that the higher the agitation, the lower the film surrounding the catalyst. That is, the species present less resistance to travel from the fluid to the particle surface or vice versa. Figure 10 shows the variation of the initial reaction rate for the different compounds as a function of the agitation studied.

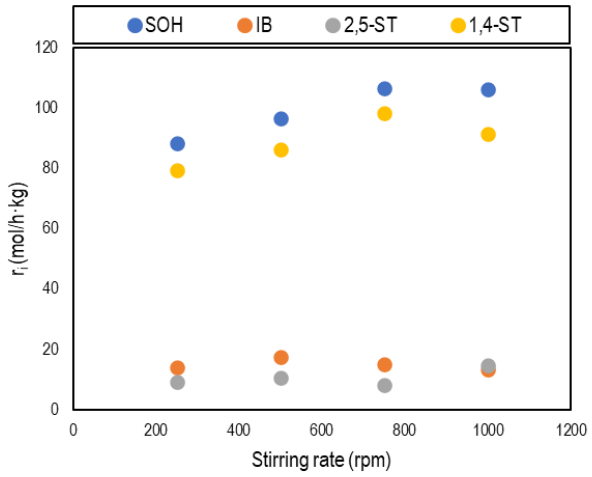

FIGURE 10. Effect of ETM on the initial reaction rate (0.75 g CT-482, 4.5 g SOH, 190 ºC and 0.16 – 0.25 mm).

It was observed that at low stirring speeds the effect of ETM was significant. However, as the agitation was increased, the rate of isosorbide formation stabilized around 750 rpm. Therefore, it was decided to work at 750 rpm.

Another condition to take into account is the catalyst load that is used to accelerate the reaction. The higher the amount of ion exchange resin, the faster the reaction takes place. Therefore, we proceeded to study the effect of the catalyst loading on the reaction rate. Figure 11 shows the variation of the reaction rate versus the load of CT-482 resin injected.

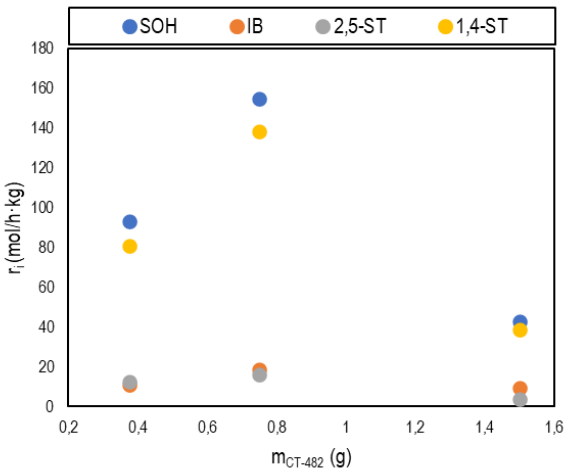

FIGURE 11. Effect of catalyst load on initial reaction rate (4.5 g SOH, 190 ºC, 0.16 – 0.25 mm and 750 rpm).

There was indeed an increase in reaction rate with increasing catalytic load. However, for very high concentrations of CT-482 a decrease in rate occurred. This could have been caused by agglomeration of the catalytic solids or by an inadequate suspension of that high mass of catalyst that resulted in mass transfer limitations between the liquid and solid phases. Because of this it was decided to use a catalytic load of 0.75 g of CT-482.

In summary, it was decided to work with a particle diameter of 0.16 - 0.25 mm, at a stirring speed of 750 rpm and 0.75 g of catalyst in order to minimize the effects of ITM, ETM and catalytic load.

5.3. REACTANTS CONVERSION, SELECTIVITY AND YIELD TOWARD TARGET PRODUCTS

After determining the conditions at which the effects of mass transfers are not governing the kinetics, the experimental design for the kinetic study of the reaction system was executed at such conditions. The study was carried out at different initial concentrations of sorbitol and several operating temperatures to grasp the effect of the experimental variables on the inherent non-linear variation of the mole evolution. A total of 15 experiments were conducted. The conversion of sorbitol, its selectivity and yield towards the target product and the rest of species were calculated. Figure 12 shows the evolution of sorbitol conversion versus time for the different operating temperatures. The representations are based on each of the initial sorbitol concentrations evaluated.

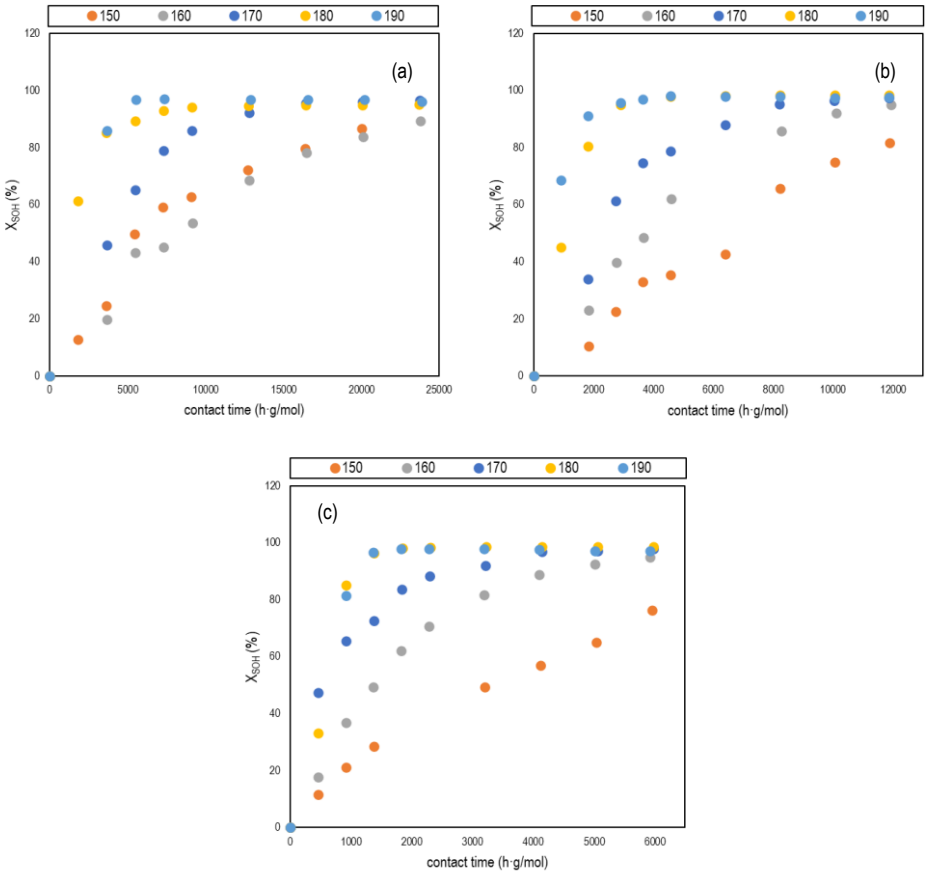

FIGURE 12. Sorbitol conversion at different temperatures (a) 2.25 g SOH (b) 4.5 g SOH (c) 9 g SOH (0.75 g CT-482, 0.16 – 0.25 mm and 750 rpm)

As mentioned above, the operating temperature has a significant influence on the reaction rate. The conversion of sorbitol increases from 80% to 97% as the initial concentration is varied from 2.25 g to 9 g, respectively. It was observed that sorbitol is virtually consumed at high temperatures. The conversion at temperatures of 180 and 190 ºC was practically the same, therefore, working at temperatures higher than 180 ºC does not produce a significant increase in the conversion of sorbitol.

The variation of isosorbide selectivity against different working temperatures was also obtained for the three initial concentrations of sorbitol. This variation is reflected in Figure 13.

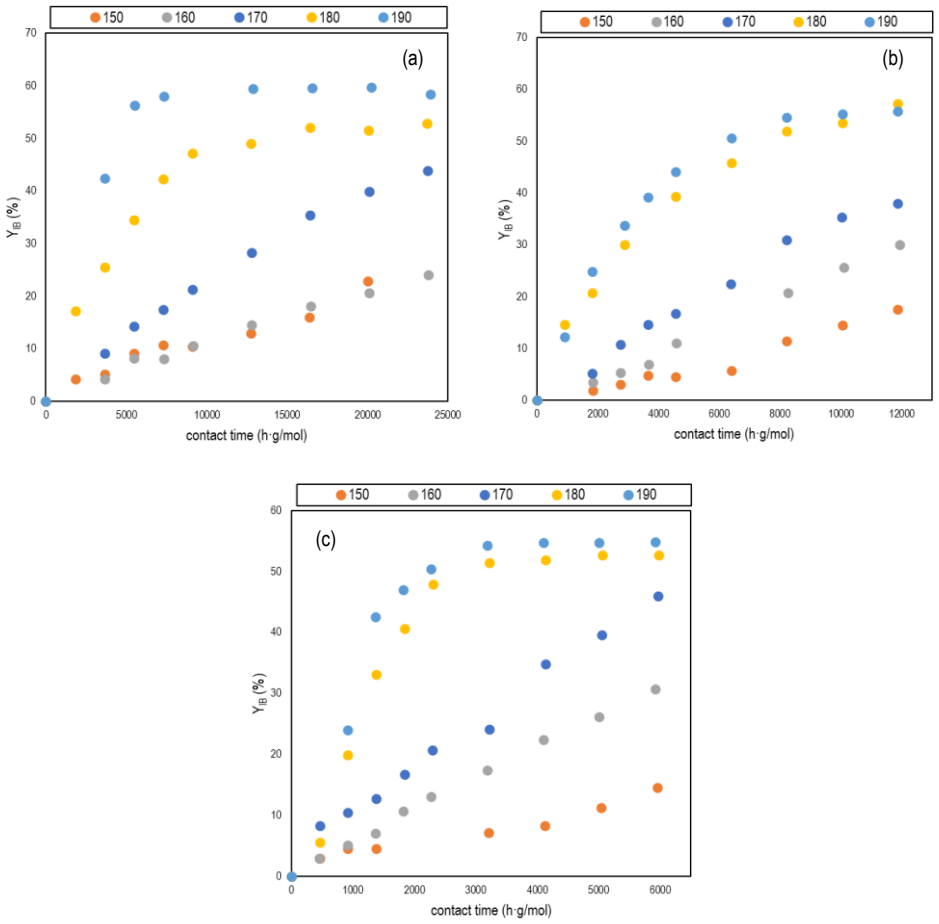

FIGURE 13. Isosorbide yield at different temperatures (a) 2.25 g SOH (b) 4.5 g SOH (c) 9 g SOH (0.75 g CT-482, 0.16 – 0.25 mm and 750 rpm)

As with sorbitol conversion, it was observed that at higher temperatures the yield increase was not as pronounced. This confirms that increasing the working temperature above 180°C will not have a significant impact on the selectivity towards isosorbide production. The yields obtained for different initial concentrations of sorbitol were also compared. It was concluded that at low temperatures the difference between yields for the three initial concentrations is greater than at high temperatures.

Table 6 summarizes the conversion, selectivity and yield values obtained at an experimental time of 6.5 hours. As expected, with increasing isosorbide yield, there was a decrease in the selectivity and yield of the intermediate product. Therefore, working at low temperatures promotes the obtaining of 1,4-sorbitan. As for 2,5-sorbitan, although its yield increases with temperature, the variation can be considered negligible compared to the increase of the target product.

TABLE 6. Final conversion, selectivity and yield values obtained from the kinetic study.

T (ºC)	m_{SOH} (g)	X_{SOH} (%)	S_{IB} (%)	$S_{1,4\text{-}ST}$ (%)	$S_{2,5\text{-}ST}$ (%)	Y_{IB} (%)	$Y_{1,4\text{-}ST}$ (%)	$Y_{2,5\text{-}ST}$ (%)
150	2.254	86.73	26.42	64.85	8.74	22.91	56.24	7.58
160	2.253	89.25	26.96	62.95	10.09	24.06	56.19	9.00
170	2.254	96.47	45.54	44.81	9.50	43.93	43.23	9.31
180	2.251	94.96	55.61	25.80	18.58	52.81	24.50	17.65
190	2.251	96.08	60.83	28.61	10.56	58.44	27.49	10.15
150	4.508	81.72	21.43	71.31	7.26	17.51	58.27	5.93
160	4.504	94.86	31.61	61.02	7.00	29.98	57.88	7.00
170	4.508	97.44	38.97	50.86	9.91	37.97	49.56	9.91
180	4.510	98.29	58.21	32.20	9.59	57.22	31.65	9.42
190	4.577	98.62	57.83	33.57	8.48	57.04	33.11	8.48
150	9.012	76.24	19.07	72.11	8.82	14.54	54.97	6.72
160	9.013	94.92	32.31	60.18	7.51	30.67	57.12	7.13
170	9.002	97.83	47.01	44.14	8.86	45.99	43.18	8.66
180	9.012	98.61	53.42	37.77	8.85	52.68	37.25	8.68
190	9.026	97.00	56.57	35.97	7.46	54.88	34.89	7.23

5.4. ESTIMATION OF EXPERIMETNAL REACTION RATE

Using the procedure described in the calculations section, the experimental reaction rates of formation or consumption of the species involved were estimated. Examples of their values with the course of the runs can be seen in Figure 14. In it, it was observed how working at higher initial concentration increases the magnitudes of the reaction rates. At initial concentrations of 2.25 g of sorbitol, the initial velocity of sorbitol was 23.81 mol h-1 kg-1 while at 9 g it reaches a value of 119.28 mol h-1 kg-1. The same happens for isosorbide, which goes from presenting a magnitude of 3.19 to 6.36 mol h-1 kg-1. It was also observed how the reaction rates decrease with time. Sorbitol presented an exponential type decrease while isosorbide was more of a linear type.

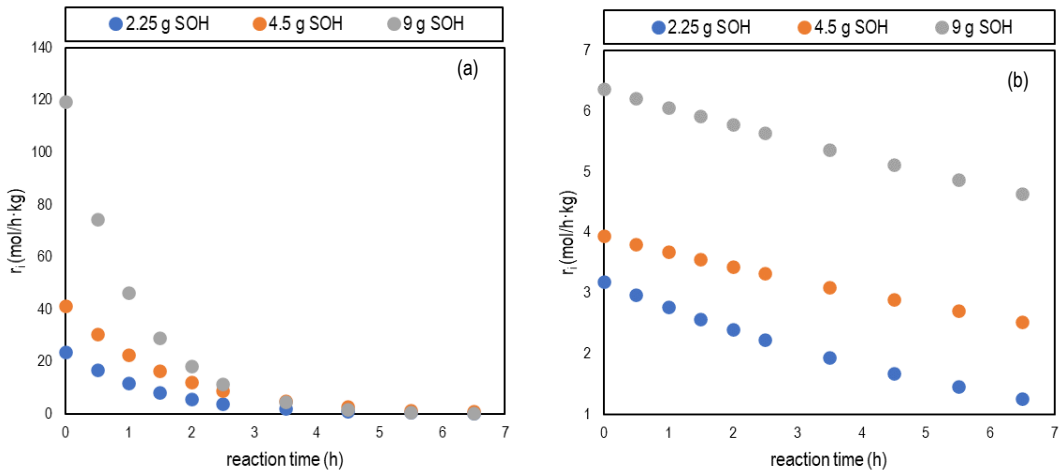

FIGURE 14. Effect of initial concentration on reaction rate (a) sorbitol (b) isosorbide (170 ºC, 0.75 g CT-482, 0.16 – 0.25 mm and 750 rpm).

Comparing the results for the three initial concentrations evaluated, it was observed that the higher the concentration, the greater the variation of the reaction rate, i.e., the more the reaction accelerates. For sorbitol the consumption is very high at high initial concentrations. However, the lower the initial reactant loading the less steep the slope of the rate becomes. In the case of isosorbide, this variation is practically not observed.

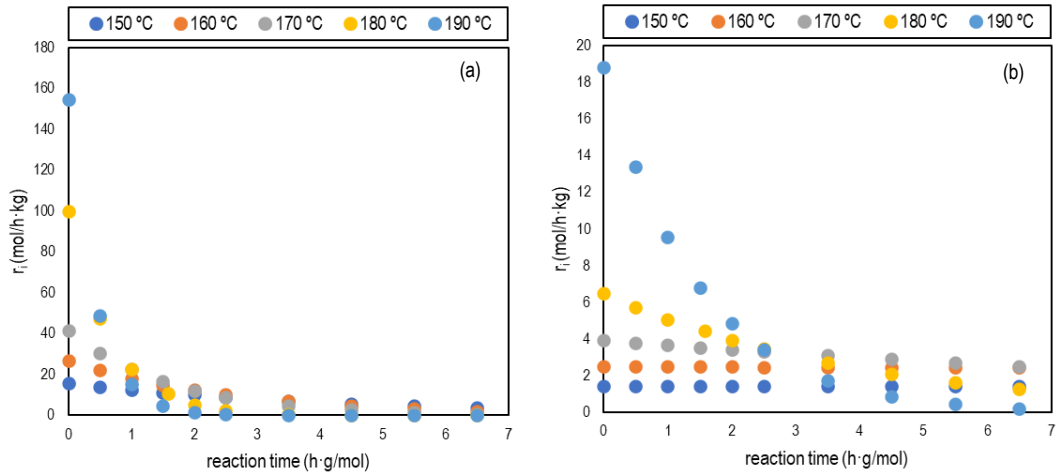

FIGURE 15. Effect of temperature on reaction rate (a) sorbitol (b) isosorbide (170 ºC, 0.75 g CT-482, 0.16 – 0.25 mm, 4.5 g SOH and 750 rpm).

On the other hand, the reaction rates of sorbitol and isosorbide were compared at different temperatures, an example is shown in Figure 15. Again, it was demonstrated that working at high temperatures accelerates the reaction. In the case of sorbitol, at 190 ºC there is a drastic decrease in the first instants of the reaction, contrary to what happens at 150 ºC, where the slope of the velocity is practically linear. The same happens for isosorbide, at high temperatures the slope is

steeper and decreases as the temperature decreases. It was also concluded that the initial velocity of both substances increases with temperature.

On the other hand, the reaction rates of sorbitol and isosorbide were compared at different temperatures, an example is shown in Figure 15. Again, it was shown that working at high temperatures accelerates the reaction. In the case of sorbitol, at 190 ºC there is a drastic decrease in the first instants of the reaction, contrary to what happens at 150 ºC, where the slope of the velocity is practically linear. The same happens for isosorbide, at high temperatures the slope is steeper and decreases as the temperature decreases. For the magnitudes of R1 and R2 obtained, it was observed that the rate of sorbitol consumption appeared to be much faster than that of isosorbide formation. This implied that the rate-determining-step was the second dehydration. It was also concluded that the initial velocities of both substances increased with temperature.

5.5. KINETIC MODELLING

Once the experimental reaction rates at different temperatures and initial sorbitol concentration were estimated from all the experiments of the kinetic study, several models based on the LHHW and ER formalisms previously mentioned were fitted to the experimental data. For this it was necessary to define the hypotheses that would lead to determine the models to be tested. It was considered that the reaction mechanism was pseudo-first order and that the limiting stage of the reaction corresponded to the surface reaction. In addition, the adsorption term was considered to be the same for the three functions to be optimized because it only depends on the composition and working temperature. The rates of the different species that were fitted simultaneously are: i) consumption of sorbitol ($-r_{SOH}$) – accounting for the formation of the intermediate 1,4-sorbitan and the byproduct 2,5-sorbitan, ii) the production of isosorbide through the dehydration of 1,4-sorbitan (r_{IB}) and, iii) the formation of the byproduct 2,5-sorbitan ($r_{2,5\text{-}ST}$). Please note that the rate of reaction R1 can be obtained as ($-r_{SOH} - r_{2,5\text{-}ST}$). Based on the recent study[34], R1 and R3 were considered irreversible and R2 as reversible so that the different driving forces originated the following kinetic expressions:

$$-r_{SOH} = \frac{(k_1 + k_3)C_{SOH}}{\{Adsorption\ term\}^{n_i}} \qquad \textit{(Eq. 5.5.1)}$$

$$r_{IB} = \frac{k_2 \cdot \left(C_{1,4-ST} - \frac{C_{IB}}{K_2}\right)}{\{Adsorption\ term\}^{n_i}} \qquad \textit{(Eq. 5.5.2)}$$

$$r_{2,5-ST} = \frac{k_3 \cdot C_{SOH}}{\{Adsorption\ term\}^{n_i}} \qquad \textit{(Eq. 5.5.3)}$$

Where the adsorption term is a function of the model and the following scenarios were envisaged for its formulation :

- The fraction of unoccupied sites can be considered to be significant or not, i.e., the *α* term is 1 or 0. Model A being in the case that it is considered relevant or B if it can be disregarded.
- The involved number of active sites can be different (1, 2 or 3, typically): this was considered by the exponent to which the adsorption term was raised to.
- Whether the adsorption contribution of a given species is considered significant or not. At this point, different scenarios depending on the number of species to be adsorbed were considered.

As a result, the models summarized in tables 7, 8, 9 and 10 were fitted to the experimental rate data previously determined.

TABLE 7. All species contribute to the adsorption term.

MODEL	$\{\boldsymbol{Adsorption\ term}\}^{n_i}$
A1	$\left(1 + K_{SOH} \cdot C_{SOH} + K_{1,4-ST} \cdot C_{1,4-ST} + K_{2,5-ST} \cdot C_{2,5-ST} + K_{IB} \cdot C_{IB} + K_W \cdot C_W\right)$
A2	$\left(1 + K_{SOH} \cdot C_{SOH} + K_{1,4-ST} \cdot C_{1,4-ST} + K_{2,5-ST} \cdot C_{2,5-ST} + K_{IB} \cdot C_{IB} + K_W \cdot C_W\right)^2$
A3	$\left(1 + K_{SOH} \cdot C_{SOH} + K_{1,4-ST} \cdot C_{1,4-ST} + K_{2,5-ST} \cdot C_{2,5-ST} + K_{IB} \cdot C_{IB} + K_W \cdot C_W\right)^3$
B1	$\left(K_{SOH} \cdot C_{SOH} + K_{1,4-ST} \cdot C_{1,4-ST} + K_{2,5-ST} \cdot C_{2,5-ST} + K_{IB} \cdot C_{IB} + K_W \cdot C_W\right)$
B2	$\left(K_{SOH} \cdot C_{SOH} + K_{1,4-ST} \cdot C_{1,4-ST} + K_{2,5-ST} \cdot C_{2,5-ST} + K_{IB} \cdot C_{IB} + K_W \cdot C_W\right)^2$
B3	$\left(K_{SOH} \cdot C_{SOH} + K_{1,4-ST} \cdot C_{1,4-ST} + K_{2,5-ST} \cdot C_{2,5-ST} + K_{IB} \cdot C_{IB} + K_W \cdot C_W\right)^3$

TABLE 8. Four species contribute to the adsorption term.

MODEL	$\{\boldsymbol{Adsorption\ term}\}^{n_i}$
A4	$\left(1 + K_{1,4-ST} \cdot C_{1,4-ST} + K_{2,5-ST} \cdot C_{2,5-ST} + K_{IB} \cdot C_{IB} + K_W \cdot C_W\right)$
A5	$\left(1 + K_{SOH} \cdot C_{SOH} + K_{2,5-ST} \cdot C_{2,5-ST} + K_{IB} \cdot C_{IB} + K_W \cdot C_W\right)$
A6	$\left(1 + K_{SOH} \cdot C_{SOH} + K_{1,4-ST} \cdot C_{1,4-ST} + K_{IB} \cdot C_{IB} + K_W \cdot C_W\right)$
A7	$\left(1 + K_{SOH} \cdot C_{SOH} + K_{1,4-ST} \cdot C_{1,4-ST} + K_{2,5-ST} \cdot C_{2,5-ST} + K_W \cdot C_W\right)$
A8	$\left(1 + K_{SOH} \cdot C_{SOH} + K_{1,4-ST} \cdot C_{1,4-ST} + K_{2,5-ST} \cdot C_{2,5-ST} + K_{IB} \cdot C_{IB}\right)$
B4	$\left(K_{1,4-ST} \cdot C_{1,4-ST} + K_{2,5-ST} \cdot C_{2,5-ST} + K_{IB} \cdot C_{IB} + K_W \cdot C_W\right)$
B5	$\left(K_{SOH} \cdot C_{SOH} + K_{2,5-ST} \cdot C_{2,5-ST} + K_{IB} \cdot C_{IB} + K_W \cdot C_W\right)$
B6	$\left(K_{SOH} \cdot C_{SOH} + K_{1,4-ST} \cdot C_{1,4-ST} + K_{IB} \cdot C_{IB} + K_W \cdot C_W\right)$
B7	$\left(K_{SOH} \cdot C_{SOH} + K_{1,4-ST} \cdot C_{1,4-ST} + K_{2,5-ST} \cdot C_{2,5-ST} + K_W \cdot C_W\right)$
B8	$\left(K_{SOH} \cdot C_{SOH} + K_{1,4-ST} \cdot C_{1,4-ST} + K_{2,5-ST} \cdot C_{2,5-ST} + K_{IB} \cdot C_{IB}\right)$

TABLE 9. Three species contribute to the adsorption term.

MODEL	$\{\boldsymbol{Adsorption\ term}\}^{n_i}$
A9	$\left(1 + K_{2,5-ST} \cdot C_{2,5-ST} + K_{IB} \cdot C_{IB} + K_W \cdot C_W\right)$
A10	$\left(1 + K_{1,4-ST} \cdot C_{1,4-ST} + K_{IB} \cdot C_{IB} + K_W \cdot C_W\right)$
A11	$\left(1 + K_{1,4-ST} \cdot C_{1,4-ST} + K_{2,5-ST} \cdot C_{2,5-ST} + K_W \cdot C_W\right)$
A12	$\left(1 + K_{1,4-ST} \cdot C_{1,4-ST} + K_{2,5-ST} \cdot C_{2,5-ST} + K_{IB} \cdot C_{IB}\right)$
A13	$\left(1 + K_{SOH} \cdot C_{SOH} + K_{IB} \cdot C_{IB} + K_W \cdot C_W\right)$
A14	$\left(1 + K_{SOH} \cdot C_{SOH} + K_{2,5-ST} \cdot C_{2,5-ST} + K_W \cdot C_W\right)$
A15	$\left(1 + K_{SOH} \cdot C_{SOH} + K_{2,5-ST} \cdot C_{2,5-ST} + K_{IB} \cdot C_{IB}\right)$
A16	$\left(1 + K_{SOH} \cdot C_{SOH} + K_{1,4-ST} \cdot C_{1,4-ST} + K_W \cdot C_W\right)$
A17	$\left(1 + K_{SOH} \cdot C_{SOH} + K_{1,4-ST} \cdot C_{1,4-ST} + K_{IB} \cdot C_{IB}\right)$
A18	$\left(1 + K_{SOH} \cdot C_{SOH} + K_{1,4-ST} \cdot C_{1,4-ST} + K_{2,5-ST} \cdot C_{2,5-ST}\right)$
B9	$\left(K_{2,5-ST} \cdot C_{2,5-ST} + K_{IB} \cdot C_{IB} + K_W \cdot C_W\right)$
B10	$\left(K_{1,4-ST} \cdot C_{1,4-ST} + K_{IB} \cdot C_{IB} + K_W \cdot C_W\right)$
B11	$\left(K_{1,4-ST} \cdot C_{1,4-ST} + K_{2,5-ST} \cdot C_{2,5-ST} + K_W \cdot C_W\right)$
B12	$\left(K_{1,4-ST} \cdot C_{1,4-ST} + K_{2,5-ST} \cdot C_{2,5-ST} + K_{IB} \cdot C_{IB}\right)$
B13	$\left(K_{SOH} \cdot C_{SOH} + K_{IB} \cdot C_{IB} + K_W \cdot C_W\right)$
B14	$\left(K_{SOH} \cdot C_{SOH} + K_{2,5-ST} \cdot C_{2,5-ST} + K_W \cdot C_W\right)$
B15	$\left(K_{SOH} \cdot C_{SOH} + K_{2,5-ST} \cdot C_{2,5-ST} + K_{IB} \cdot C_{IB}\right)$
B16	$\left(K_{SOH} \cdot C_{SOH} + K_{1,4-ST} \cdot C_{1,4-ST} + K_W \cdot C_W\right)$
B17	$\left(K_{SOH} \cdot C_{SOH} + K_{1,4-ST} \cdot C_{1,4-ST} + K_{IB} \cdot C_{IB}\right)$
B18	$\left(K_{SOH} \cdot C_{SOH} + K_{1,4-ST} \cdot C_{1,4-ST} + K_{2,5-ST} \cdot C_{2,5-ST}\right)$

TABLE 10. Two species contribute to the adsorption term.

MODEL	$\{\boldsymbol{Adsorption\ term}\}^{n_i}$
A19	$\left(1 + K_{SOH} \cdot C_{SOH} + K_{1,4-ST} \cdot C_{1,4-ST}\right)$
A20	$\left(1 + K_{SOH} \cdot C_{SOH} + K_{2,5-ST} \cdot C_{2,5-ST}\right)$
A21	$\left(1 + K_{SOH} \cdot C_{SOH} + K_{IB} \cdot C_{IB}\right)$
A22	$\left(1 + K_{SOH} \cdot C_{SOH} + K_{W} \cdot C_{W}\right)$
A23	$\left(1 + K_{1,4-ST} \cdot C_{1,4-ST} + K_{2,5-ST} \cdot C_{2,5-ST}\right)$
A24	$\left(1 + K_{1,4-ST} \cdot C_{1,4-ST} + K_{IB} \cdot C_{IB}\right)$
A25	$\left(1 + K_{1,4-ST} \cdot C_{1,4-ST} + K_{W} \cdot C_{W}\right)$
A26	$\left(1 + K_{2,5-ST} \cdot C_{2,5-ST} + K_{IB} \cdot C_{IB}\right)$
A27	$\left(1 + K_{2,5-ST} \cdot C_{2,5-ST} + K_{W} \cdot C_{W}\right)$
A28	$\left(1 + K_{IB} \cdot C_{IB} + K_{W} \cdot C_{W}\right)$
B19	$\left(K_{SOH} \cdot C_{SOH} + K_{1,4-ST} \cdot C_{1,4-ST}\right)$
B20	$\left(K_{SOH} \cdot C_{SOH} + K_{2,5-ST} \cdot C_{2,5-ST}\right)$
B21	$\left(K_{SOH} \cdot C_{SOH} + K_{IB} \cdot C_{IB}\right)$
B22	$\left(K_{SOH} \cdot C_{SOH} + K_{W} \cdot C_{W}\right)$
B23	$\left(K_{1,4-ST} \cdot C_{1,4-ST} + K_{2,5-ST} \cdot C_{2,5-ST}\right)$
B24	$\left(K_{1,4-ST} \cdot C_{1,4-ST} + K_{IB} \cdot C_{IB}\right)$
B25	$\left(K_{1,4-ST} \cdot C_{1,4-ST} + K_{W} \cdot C_{W}\right)$
B26	$\left(K_{2,5-ST} \cdot C_{2,5-ST} + K_{IB} \cdot C_{IB}\right)$
B27	$\left(K_{2,5-ST} \cdot C_{2,5-ST} + K_{W} \cdot C_{W}\right)$
B28	$\left(K_{IB} \cdot C_{IB} + K_{W} \cdot C_{W}\right)$

After defining the models to be tested, the evaluation of their fitting goodness was assessed by means of the total sum of squared residuals (sum of the 3 reactions fitted simultaneously) and by the evaluation of the corresponding parity and residuals plot. Table 11 summarizes the parameters estimated for all the models evaluated along with their RSS.

In general terms, after assessing the whole of models evaluated, it was observed that type A models, those in which the fraction of unoccupied sites is considered relevant (α = 1), fitted more reliably the experimental data obtained. Moreover, those models where sorbitol is considered to be one of the adsorbed species, it was observed that the first term of the adsorption constant tended to zero. This fact is explained by the fact that, at high reaction times, sorbitol is practically completely consumed, so that the iterative system has to give more weight to the rest of the parameters involved. The solution to this problem would be to consider that the adsorption terms are different for the different reactions evaluated.

De los modelos tipo A, los dos que mejor se ajustan a los valores experimentales son el A11 y A4, con un valor de suma cuadrática de residuos de $1.003 \cdot 10^4$ y $1.004 \cdot 10^4$, respectivamente.

Los gráficos de paridad y de residuos para los dos mejores modelos obtenidos se representan en la Figura 16. Los correspondientes a todos los modelos evaluados se incluyen en el Apéndice 3.

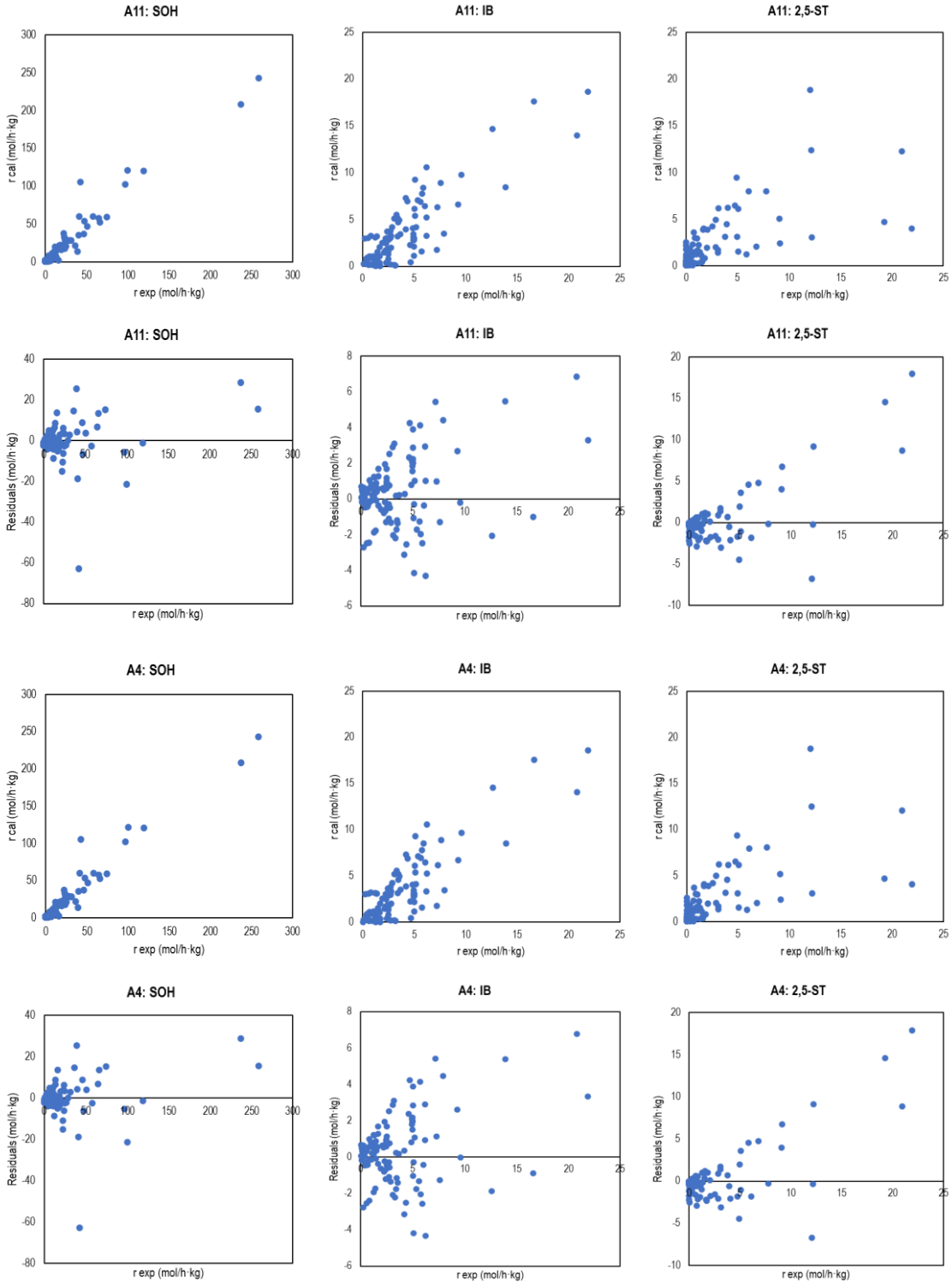

FIGURE 16. The parity and residuals distribution for the two best models obtained, A11 and A4.

As can be seen in Figure 16, the parity plot for both models fit best for the rate of sorbitol consumption. This is because equal importance has been given to the three reactions by optimizing for the reaction rate values with the highest weights. These velocities coincide with those of sorbitol in the first instants of the reaction. A possible solution would be to indicate the importance of each equation so that the parameters are adjusted according to the isosorbide formation rate, since this is the objective function. On the residual plot, a good random dispersion is observed for the 3 species with the exception of certain experiments. Even so, the fit can be considered as good considering that it corresponds to an approximate study from which to start.

TABLE 11. Los Estimated parameters together with their RSS for the 56 models analyzed.

MODEL	n	k_1	$k_{T,1}$	k_2	$k_{T,2}$	k_3	$k_{T,3}$	K_{2eq1}	K_{2eqT}	$K_{SOH,1}$	$K_{SOH,T}$	$K_{1,4\text{-}ST,1}$	$K_{1,4\text{-}ST,T}$	$K_{2,5\text{-}ST,1}$	$K_{2,5\text{-}ST,T}$	$K_{IB,1}$	$K_{IB,T}$	$K_{W,1}$	$K_{W,T}$	RSS_i
A1	1	10.33	-17805	9.52	-21569	7.16	-8367	0.67	-3295	0.00	-2409	0.00	-2421	7.89	-38664	4.47	-579	2.44	-10319	2.105E+04
A2	2	9.97	-17960	9.09	-21570	6.49	-8347	0.70	-3296	0.00	-2411	1.43	-2422	5.56	-38659	2.13	-581	0.67	-10173	1.841E+04
A3	3	8.78	-17013	7.95	-21547	5.38	-8346	0.65	-3285	0.00	-24156	2.66	-24243	4.04	-38666	0.00	-5889	0.00	-101586	3.804E+04
A4	1	8.43	-14800	7.79	-21514	5.64	-8329	0.64	-3274	-	-	3.03	-24264	6.26	-38667	0.00	-5009	0.27	-101637	1.004E+04
A5	1	8.47	-15016	7.88	-23026	5.55	-7246	0.64	-1822	0.00	-18385	-	-	6.63	-35632	1.39	-7359	0.27	-116994	1.049E+04
A6	1	8.47	-14588	7.34	-14806	5.83	-10126	0.55	-1033	0.00	-31937	2.99	-6566	-	-	1.01	-2019	0.35	-64265	1.141E+04
A7	1	9.25	-12401	8.53	-17204	6.75	-9811	0.76	-7381	0.00	-11432	5.44	-64511	4.30	-11230	-	-	1.23	-5087	2.120E+04
A8	1	8.21	-12370	7.50	-17207	5.69	-9800	0.78	-7383	2.33	-117431	4.67	-64509	4.58	-11232	0.00	-50370	-	-	1.609E+04
A9	1	8.42	-14647	7.91	-23812	5.68	-8937	0.70	-4592	-	-	-	-	6.63	-35635	0.00	-7369	0.26	-116994	1.009E+04
A10	1	8.47	-15009	7.79	-20753	5.67	-8369	0.97	-3475	-	-	1.47	-5749	-	-	5.59	-32129	0.34	-71266	1.051E+04
A11	1	8.42	-14716	7.79	-21719	5.65	-8449	0.63	-3122	-	-	3.04	-22880	6.29	-40568	-	-	0.26	-118459	1.003E+04
A12	1	7.74	-8537	7.18	-16091	5.34	-7440	0.77	-5870	-	-	2.21	-19565	0.00	-27296	4.82	-299832	-	-	2.191E+04
A13	1	8.50	-15097	7.93	-22692	5.70	-8248	1.05	-3377	0.00	-3628	-	-	-	-	5.73	-27179	0.35	-299983	1.102E+04
A14	1	8.61	-16045	7.89	-21991	5.78	-8926	0.65	-3196	0.00	-15368	-	-	6.43	-27849	-	-	0.53	-57389	1.066E+04
A15	1	8.10	-11207	7.65	-22570	5.55	-8115	0.64	-2135	1.81	-31096	-	-	6.25	-37293	3.80	-299972	-	-	1.988E+04
A16	1	8.44	-14974	7.81	-22474	5.64	-8242	0.56	-2021	0.00	-31017	4.55	-37367	-	-	-	-	0.24	-299983	1.053E+04
A17	1	8.21	-12498	7.67	-20823	5.67	-9903	0.65	-3627	2.33	-171914	4.68	-49057	-	-	3.13	-21491	-	-	1.599E+04
A18	1	8.22	-12541	7.65	-20651	5.69	-10035	0.65	-3446	2.35	-175041	3.59	-43590	6.32	-42951	-	-	-	-	1.591E+04
A19	1	8.21	-12502	7.65	-20798	5.67	-9931	0.61	-3528	2.33	-155081	4.76	-47910	-	-	-	-	-	-	1.600E+04
A20	1	8.22	-12546	7.65	-20786	5.68	-9955	0.68	-3379	2.35	-155407	-	-	6.71	-42221	-	-	-	-	1.593E+04
A21	1	8.21	-12508	7.79	-22550	5.68	-9940	1.17	-6118	2.34	-461948	-	-	-	-	5.92	-38381	-	-	1.634E+04
A22	1	8.28	-13772	6.92	-13979	5.50	-7616	0.57	-3118	0.00	-81120	-	-	-	-	-	-	0.02	-116432	1.442E+04
A23	1	7.74	-8580	7.18	-16555	5.33	-7444	0.62	-4008	-	-	4.00	-83654	3.36	-21744	-	-	-	-	2.168E+04
A24	1	7.74	-8587	7.14	-16113	5.34	-7483	0.60	-3184	-	-	4.01	-61575	-	-	0.00	-27701	-	-	2.166E+04
A25	1	8.28	-13700	7.35	-19378	5.56	-8280	0.61	-3724	-	-	4.11	-151764	-	-	-	-	0.00	-82580	1.318E+04
A26	1	7.74	-8584	7.13	-16114	5.33	-7454	0.71	-4471	-	-	-	-	5.89	-161015	2.96	-24194	-	-	2.168E+04
A27	1	8.28	-13729	7.41	-20749	5.58	-8475	0.58	-2511	-	-	-	-	6.09	-158300	-	-	0.01	-77676	1.315E+04
A28	1	8.28	-13745	7.34	-19374	5.57	-8278	0.72	-5413	-	-	-	-	-	-	4.88	-157982	0.03	-77908	1.347E+04

MODEL	n	k_1	$k_{T,1}$	k_2	$k_{T,2}$	k_3	$k_{T,3}$	K_{2eq1}	K_{2eqT}	$K_{SOH,1}$	$K_{SOH,T}$	$K_{1,4\text{-}ST,1}$	$K_{1,4\text{-}ST,T}$	$K_{2,5\text{-}ST,1}$	$K_{2,5\text{-}ST,T}$	$K_{IB,1}$	$K_{IB,T}$	$K_{W,1}$	$K_{W,T}$	RSS_i
B1	1	9.87	-18375	9.03	-21527	6.26	-8844	0.70	-3261	0.01	-2038	0.00	-2420	7.22	-38665	4.64	-577	2.06	-10296	2.23E+04
B2	2	9.97	-17960	9.09	-21570	6.49	-8347	0.70	-3296	0.00	-2411	1.43	-2422	5.56	-38659	2.13	-581	0.67	-10173	6.77E+04
B3	3	23.90	-12943	23.10	-21426	21.11	-7736	0.69	-3227	0.00	-245	2.28	-240	7.33	-3892	7.39	-541	5.38	-1565	2.32E+04
B4	1	11.01	-16444	10.08	-21451	7.75	-8465	0.64	-3245	-	-	0.00	-2423	0.00	-3591	6.42	-457	3.25	-8553	2.30E+04
B5	1	8.53	-14880	7.46	-23103	4.76	-10142	1.11	-3560	3.06	-5093	-	-	6.17	-35333	4.95	-2067	0.27	-67083	5.44E+04
B6	1	8.01	-14585	7.45	-14804	6.11	-10109	0.91	-10613	3.65	-14489	2.94	-6422	-	-	1.01	-2019	0.35	-64265	1.08E+05
B7	1	14.69	-13826	13.65	-20129	12.22	-10142	0.63	-7310	0.00	-1162	9.07	-6534	0.00	-1121	-	-	6.94	-4964	2.36E+04
B8	1	5.17	-13919	4.46	-20115	3.01	-14789	1.03	-7364	0.37	-6968	0.00	-15112	1.15	-1240	1.88	-5160	-	-	7.07E+04
B9	1	7.94	-14619	6.94	-20689	6.18	-8312	0.59	-3452	-	-	-	-	0.00	-341	2.89	-383	0.18	-249	3.81E+04
B10	1	10.04	-12948	9.28	-20621	7.30	-8194	0.71	-3423	-	-	0.00	-3406	-	-	5.97	-3883	2.29	-4811	2.30E+04
B11	1	7.77	-14634	6.70	-21336	5.73	-8362	0.52	-3345	-	-	0.67	-2282	3.01	-3848	-	-	0.00	-2651	2.98E+04
B12	1	6.91	-17406	17.59	-15379	5.21	-10371	1.02	-3356	-	-	15.46	-9459	0.36	-13848	0.00	-12650	-	-	5.90E+04
B13	1	15.53	-12008	14.76	-22610	12.84	-7536	0.67	-3341	0.00	-396	-	-	-	-	11.33	-353	7.79	-4061	2.30E+04
B14	1	13.80	-7995	12.93	-22187	11.43	-7200	0.53	-2917	0.00	-833	-	-	10.41	-313	-	-	6.08	-299	2.32E+04
B15	1	4.69	-8008	4.28	-22570	2.63	-8119	0.71	-2135	0.00	-3097	-	-	2.72	-3721	0.79	-2971	-	-	7.34E+04
B16	1	7.82	-23491	6.34	-21001	2.06	-9543	0.59	-2609	0.69	-8099	1.76	-3795	-	-	-	-	0.01	-22551	2.63E+04
B17	1	4.84	-10807	4.49	-21081	2.59	-9544	0.80	-2666	0.00	-2627	0.61	-4549	-	-	2.05	-22490	-	-	7.21E+04
B18	1	4.89	-12539	3.92	-20651	2.86	-10034	0.59	-3446	0.00	-1754	0.20	-4351	1.90	-1250	-	-	-	-	7.68E+04
B19	1	4.80	-7361	3.91	-10252	2.53	-5575	0.60	-1143	0.00	-230	1.04	-494	-	-	-	-	-	-	7.33E+04
B20	1	4.81	-8872	3.75	-16806	2.61	-8328	0.87	-9692	0.00	-1842	-	-	2.71	-1361	-	-	-	-	7.14E+04
B21	1	4.82	-15743	4.01	-19575	2.50	-13351	1.97	-6294	0.00	-8483	-	-	-	-	2.12	-7148	-	-	7.07E+04
B22	1	14.21	-13291	12.95	-14989	11.73	-11093	0.58	-4873	0.00	-13008	-	-	-	-	-	-	6.51	-4941	2.40E+04
B23	1	2.50	-18791	11.80	-20697	0.012	-17187	0.904	-4513	-	-	10.383	-83937	10.299	-5846	-	-	-	-	4.58E+04
B24	1	2.43	-22165	6.06	-19748	0.00	-8477	8.14	-40651	-	-	10.47	-84491	-	-	10.26	-5744	-	-	5.06E+04
B25	1	7.72	-15004	6.71	-17548	5.35	-14280	0.54	-3065	-	-	2.24	-8246	-	-	-	-	0.00	-7099	2.28E+04
B26	1	1.83	-22315	2.32	-22587	0.04	-15506	2.20	-4070	-	-	-	-	7.68	-84489	10.02	-5709	-	-	7.16E+04
B27	1	7.72	-15277	6.64	-16009	5.33	-14263	0.59	-2634	-	-	-	-	4.41	-8570	-	-	0.00	-7579	2.25E+04
B28	1	7.73	-15545	6.71	-16537	5.33	-14384	0.83	-2674	-	-	-	-	-	-	3.68	-7890	0.00	-7577	2.26E+04

As mentioned above, the best fitting models are model A11 and A4. In model A11 it is considered that the species that contribute significantly to the adsorption term are: 1,4-sorbitan, 1,5-sorbitan and water. Considering that the work was carried out in an aqueous medium and that the resins are hygroscopic in nature, it makes sense that water would influence the adsorption term. On the other hand, 1,5-sorbitan is present in most of the reaction time and influences the isosorbide selectivity. Furthermore, the contribution of 1,4-sorbitan to the adsorption term would justify the slowdown towards isosorbide formation, making reaction R2 the rate-determining step. The functions of the reaction equations would be as follows:

$$-r_{SOH} = \frac{(k_1 + k_3)C_{SOH}}{\left(1 + K_{1,4-ST} \cdot C_{1,4-ST} + K_{2,5-ST} \cdot C_{2,5-ST} + K_W \cdot C_W\right)} \quad \textit{(Eq. 5.5.4)}$$

$$r_{IB} = \frac{k_2 \cdot \left(C_{1,4-ST} - \frac{C_{IB}}{K_2}\right)}{\left(1 + K_{1,4-ST} \cdot C_{1,4-ST} + K_{2,5-ST} \cdot C_{2,5-ST} + K_W \cdot C_W\right)} \quad \textit{(Eq. 5.5.5)}$$

$$r_{2,5-ST} = \frac{k_3 \cdot C_{SOH}}{\left(1 + K_{1,4-ST} \cdot C_{1,4-ST} + K_{2,5-ST} \cdot C_{2,5-ST} + K_W \cdot C_W\right)} \quad \textit{(Eq. 5.5.6)}$$

On the other hand, in model 4, the above species plus isosorbide are adsorbed. In this one, the target product would also be rate limiting. This together with the resistance of the 1,4-sorbitan to adsorb makes the second dehydration slow compared to the first. However, the parameter $K_{IB,1}$ tended to zero. This may be due to the fact that in the first instants of the reaction there is practically no isosorbide concentration. It is at these times that the reaction rate is at its greatest magnitude, causing the iterative system to prioritize other parameters. This problem would be solved by giving the same level of priority to the optimization of all the reaction rates and not prioritizing those of greater magnitude as has been done for the moment. The functions of the three reactions studied for model A4 are shown below:

$$-r_{SOH} = \frac{(k_1 + k_3)C_{SOH}}{\left(1 + K_{1,4-ST} \cdot C_{1,4-ST} + K_{2,5-ST} \cdot C_{2,5-ST} + K_{IB} \cdot C_{IB} + K_W \cdot C_W\right)} \quad \textit{(Eq. 5.5.7)}$$

$$r_{IB} = \frac{k_2 \cdot \left(C_{1,4-ST} - \frac{C_{IB}}{K_2}\right)}{\left(1 + K_{1,4-ST} \cdot C_{1,4-ST} + K_{2,5-ST} \cdot C_{2,5-ST} + K_{IB} \cdot C_{IB} + K_W \cdot C_W\right)} \quad \textit{(Eq. 5.5.8)}$$

$$r_{2,5-ST} = \frac{k_3 \cdot C_{SOH}}{\left(1 + K_{1,4-ST} \cdot C_{1,4-ST} + K_{2,5-ST} \cdot C_{2,5-ST} + K_{IB} \cdot C_{IB} + K_W \cdot C_W\right)} \quad \textit{(Eq. 5.5.9)}$$

Finally, the variations of the kinetic and adsorption constants were obtained with respect to the temperature range studied. Figure 17 shows the variation of these constants for both models.

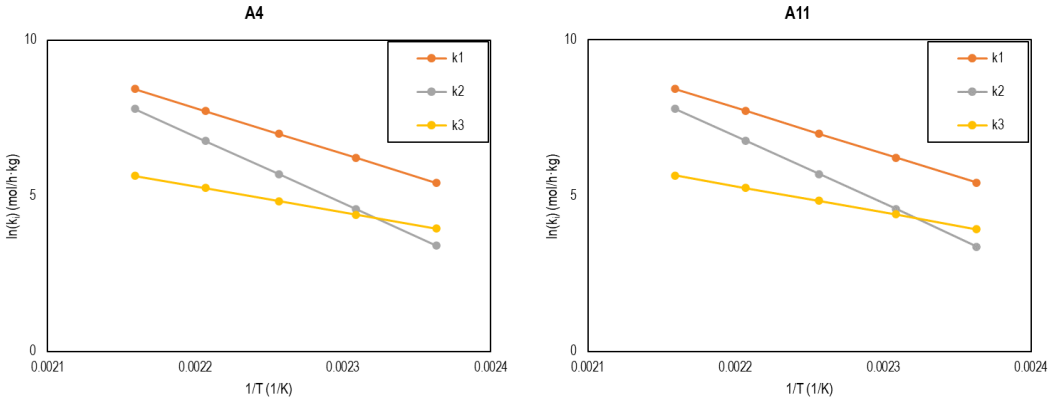

FIGURE 17. Arrhenius plot of the kinetic terms for reactions R1, R2 and R3 for models A4 and A11.

In these graphs it was observed that the kinetic constant of the reaction that shows the greatest dependence on temperature is R2 while R3 has the least influence. From the parameter $k_{i,T}$ (Eq. 4.7.7) the apparent activation energies for the three reactions were obtained ($k_{i,T} = -E_{a,i}/R$). Table 12 summarizes the energies obtained for the two models described above.

TABLE 12. Apparent activation energies for dehydration reactions.

MODEL	$E'_{a,1}$ (kJ/mol)	$E'_{a,2}$ (kJ/mol)	$E'_{a,3}$ (kJ/mol)
A4	123.1	178.9	69.2
A11	122.4	180.6	70.3

In the recently published study, the activation energy values are as follows: 117.38 kJ mol^{-1}, 137.56 kJ mol^{-1} and 139.89 kJ mol^{-1} for reactions R1, R2 and R3, respectively.[34] The activation energy values for the first two reactions show the same trend, reaction R1 has lower magnitude than R2. However, for the formation of the byproduct (R3) the activation energy value is twice the literature value. This is probably due to the generalized bad fit of R3. To solve this difference, equal importance should be given to all three reactions as discussed above. On the other hand, the parameters are generally larger due to the lack of normalization on the level of importance of the reactions and the magnitudes of reaction rates.

6. CONCLUSIONS

It was demonstrated that the synthesis of isosorbide from sorbitol in aqueous media is possible. The study was carried out in a temperature range between 150 - 190 °C from which isosorbide yields between 20 - 60 % were obtained, respectively. Furthermore, it was concluded that the reaction mechanism is composed of two dehydrations in series-parallel where, in the first reaction step, the by-product 2,5-sorbitan is generated. Its formation interferes with the yield of the target product. Of the two stages, the second dehydration would be the determining stage of the reaction.

The kinetic study was performed under experimental conditions where the effects of ETM, ITM and catalytic loading were minimal. Thus, the rate limiting stage of the reaction was the surface reaction. The reactions were considered to be pseudo first order. Furthermore, it was decided that the first dehydration stage (R1 and R3) exhibited irreversible behavior while the second dehydration was reversible. In order to obtain satisfactory kinetic models for the reaction network studied, a series of kinetic equations were proposed and fitted to the experimental data. These kinetic equations were expressed in terms of concentrations and based on the LHHW and ER formalisms. Of all the models analyzed, the models that considered the fraction of unoccupied sites relevant (model A) fitted better than those that considered it negligible (model B). Of the type A models, the two best fitting models were obtained: the one that considered that 1,4-ST, 2,5-ST and W contribute to the adsorption term and the one that considered these species plus IB. The study carried out is approximate, so the parameters obtained are considered indicative.

7. RECOMMENDATIONS FOR FUTURE WORK

- To evaluate different objective functions that can give equal relevance to the fitting of all reactions since the use one gives priority to the consumption of sorbitol.
- To perform a kinetic modelling by solving the involved differential equations of the rates of reaction considered instead of minimizing the reaction rates.
- To perform the kinetic modelling in terms of activities rather than in terms of concentrations because the involved compounds are highly non-ideal.
- To add the contribution of additional parameters, such as the resin-medium interaction, in the model equations evaluated.

8. NOTATION

K_j	Adsorption equilibrium constant of species j, dimensionless
$E'_{a,i}$	Apparent activation energy of the reaction i, kJ/mol
α	Binary parameter (value: 0, 1)
cal	Calculed
W_{cat}	Catalyst mass in dry basis, g
C_j	Concentration of species j, %
ER	Eley-Rideal
K_i	Equilibrium constant of reaction i, dimensionless
exp	Experimental
TEM	External Transfer of Matter
GHG	Greenhouse gases
HPLC	High-Performance Liquid Chromatograph
m_{SOH}	Initial sorbitol mass, g
TIM	Internal Transfer of Matter
IB	Isosorbide
k_i	Kinetic coefficient of reaction i, mol/h·kg
LHHW	Langmuir-Hinshelwood-Hougen-Watson
n_j	Number of mol of species j, mol
d_p	Particle diameter, mm
r_i	Reaction rate of species i, mol/h·kg
RSS_i	Residual sum of squares
S_j	Selectivity of species j, %
1,4 - ST	Sorbian
2,5 - ST	Sorbian
SOH	Sorbitol
X_{SOH}	Sorbitol conversion, %
$\Delta_{ads}H_j^0$	Standard molar enthalpy of adsorption of species j, kJ/mol
$\Delta_{ads}S_j^0$	Standard molar entropy of adsorption of species j, kJ/mol·K
T	Temperature, K
W	Water
Y_j	Yield of species j, %

9. REFERENCES AND NOTES

(1) *Fossil*. Department of Energy. https://www.energy.gov/science-innovation/energy-sources/fossil (accessed 2022-05-24).

(2) Kopp, O. C. *Fossil fuel*. Encyclopedia Britannica. https://www.britannica.com/science/fossil-fuel (accessed 2022-05-24).

(3) Ausfelder, F.; Bazzanella, A.; VanBracki, H.; Wilde, R.; Beckmann, C.; Mills, R.; Rightor, E.; Tam, C.; Trudeau, N.; Botschek, P. Technology Roadmap Energy and GHG Reductions in the Chemical Industry via Catalytic Processes. **2013**.

(4) Dogan, B.; Erol, D. The Future of Fossil and Alternative Fuels Used in Automotive Industry. In *3rd International Symposium on Multidisciplinary Studies and Innovative Technologies (ISMSIT)*; Institute of Electrical and Electronics Engineers: Ankara, Turkey, Turkey, **2019**. https://doi.org/10.1109/ISMSIT.2019.8932925.

(5) Bahmani, R.; Kim, D. G.; Modareszadeh, M.; Thompson, A. J.; Park, J. H.; Yoo, H. H.; Hwang, S. The Mechanism of Root Growth Inhibition by the Endocrine Disruptor Bisphenol A (BPA). *Environ. Pollut.* **2020**, *257*, 113516. https://doi.org/10.1016/j.envpol.2019.113516.

(6) Liguori, F.; Moreno-Marrodan, C.; Barbaro, P. Biomass-Derived Chemical Substitutes for Bisphenol A: Recent Advancements in Catalytic Synthesis. *Chem. Soc. Rev.* **2020**, *49* (17), 6329–6363. https://doi.org/10.1039/d0cs00179a.

(7) *Biomass*. European Commission. https://energy.ec.europa.eu/topics/renewable-energy/bioenergy/biomass_en (accessed 2022-05-14).

(8) Radlein, D.; Quignard, A. A Short Historical Review of Fast Pyrolysis of Biomass. *Oil Gas Sci. Technol.* **2013**, *68* (4), 765–783. https://doi.org/10.2516/ogst/2013162.

(9) Alonso, D. M.; Bond, J. Q.; Dumesic, J. A. Catalytic Conversion of Biomass to Biofuels. *Green Chem.* **2010**, *12* (9), 1493–1513. https://doi.org/10.1039/c004654j.

(10) Tejero, M. A.; Ramírez, E.; Fité, C.; Tejero, J.; Cunill, F. Esterification of Levulinic Acid with Butanol over Ion Exchange Resins. *Appl. Catal. A Gen.* **2016**, *517* (May), 56–66. https://doi.org/10.1016/j.apcata.2016.02.032.

(11) Bomtempo, J. V.; Chaves Alves, F.; De Almeida Oroski, F. Developing New Platform Chemicals: What Is Required for a New Bio-Based Molecule to Become a Platform Chemical in the Bioeconomy? *Faraday Discuss.* **2017**, *202*, 213–225. https://doi.org/10.1039/c7fd00052a.

(12) Bozell, J.; J.; Petersen, G. R. Technology Development for the Production of Biobased Products from Biorefinery Carbohydrates—the US Department of Energy's "Top 10" Revisited. *Green Chem.* **2010**, *12* (4), 539–554. https://doi.org/10.1039/b922014c.

(13) Chávez-Sifontes, M. La Biomasa: Fuente Alternativa de Combustibles y Compuestos Químicos. *An. Química - RSEQ* **2019**, *115* (5), 399–407.

(14) *Sorbitol-Production , Technology, Applications, Patent, Consultants, Company Profiles, Reports, Market, Projects, Guides*. Primary Information Services. http://www.primaryinfo.com/projects/sorbitol.htm (accessed 2022-05-01).

(15) Liauw, S.; Saibil, F. Sorbitol: Often Forgotten Cause of Osmotic Diarrhea. *Can. Fam. Physician* **2019**, *65* (8), 557–558.

(16) Saxon, D. J.; Luke, A. M.; Sajjad, H.; Tolman, W. B.; Reineke, T. M. Next-Generation Polymers: Isosorbide as a Renewable Alternative. *Prog. Polym. Sci.* **2020**, *101*, 1–14. https://doi.org/10.1016/j.progpolymsci.2019.101196.

(17) Aricò, F.; Tundo, P. Isosorbide and Dimethyl Carbonate: A Green Match. *Beilstein J. Org. Chem.* **2016**, *12*, 2256–2266. https://doi.org/10.3762/bjoc.12.218.

(18) Yabushita, M.; Kobayashi, H.; Shrotri, A.; Hara, K.; Ito, S.; Fukuoka, A. Sulfuric Acid-Catalyzed Dehydration of Sorbitol: Mechanistic Study on Preferential Formation of 1,4-Sorbitan. *Bull. Chem. Soc. Jpn.* **2015**, *88* (7), 996–1002. https://doi.org/10.1246/bcsj.20150080.

(19) Castro Santacreu, L. TFG: A Contribution to the Study of the Fructose to Isosorbide Conversion Reaction., Universidad de Barcelona, Barcelona, Spain, **2022**.

(20) Contreras, A. C. THESIS: Diseño de Catalizadores Heterogéneos Con Actividad Tándem Ácida/Hidrogenante Para La Producción En Una Etapa de Isosorbida a Partir de Glucosa, Escuela Internacional de Doctorado, **2020**.

(21) Dussenne, C.; Delaunay, T.; Wiatz, V.; Wyart, H.; Suisse, I.; Sauthier, M. Synthesis of Isosorbide: An Overview of Challenging Reactions. *Green Chem.* **2017**, *19*, 5332–5344. https://doi.org/10.1039/c7gc01912b.

(22) Gu, M.; Yu, D.; Zhang, H.; Sun, P.; Huang, H. Metal (IV) Phosphates as Solid Catalysts for Selective Dehydration of Sorbitol to Isosorbide. *Catal. Letters* **2009**, *133*, 214–220. https://doi.org/10.1007/s10562-009-0142-5.

(23) Alice, O.; Hoelderich, W. F.; Wyart, H.; Ibert, M. Metal Phosphate Catalyzed Dehydration of Sorbitol under Hydrothermal Conditions. *Appl. Catal. B, Environ.* **2015**, *176–177*, 139–149. https://doi.org/10.1016/j.apcatb.2015.03.033.

(24) Otomo, R.; Yokoi, T.; Tatsumi, T. Synthesis of Isosorbide from Sorbitol in Water over High-Silica Aluminosilicate Zeolites. *Appl. Catal. A, Gen.* **2015**, *505*, 28–35. https://doi.org/10.1016/j.apcata.2015.07.034.

(25) Ginés-Molina, M. J.; Moreno-Tost, R.; Santamaría-González, J.; Maireles-Torres, P. Dehydration of Sorbitol to Isosorbide over Sulfonic Acid Resins under Solvent-Free Conditions. *Appl. Catal. A, Gen.* **2017**, *537*, 66–73. https://doi.org/10.1016/j.apcata.2017.03.006.

(26) Izquierdo, J. F.; Cunill, F.; Tejero, J.; Iborra, M.; Fité, C. Reacciones Catalizadas Por Sólidos. In *Cinética de las reacciones químicas*; Edicions Universitat de Barcelona: Barcelona, **2004**; pp 143–267.

(27) Soto López, R. THESIS: Simultaneous Etherification of C4 and C5 Iso-Olefins with Ethanol over Acidic Ion-Exchange Resins for Greener Fuels, University of Barcelona, **2017**.

(28) Wheaton, R. M.; Lefevre, L. J. DOWEX Ion Exchange Resins: Fundamentals of Ion

Exchange. *Dow Liquid Separations*. pp 1–9.

(29) Ramírez, E.; Bringué, R.; Fité, C.; Iborra, M.; Tejero, J.; Cunill, F. Role of Ion-Exchange Resins as Catalyst in the Reaction-Network of Transformation of Biomass into Biofuels. *J. Chem. Technol. Biotechnol.* **2017**, *92* (11), 2775–2786. https://doi.org/10.1002/jctb.5352.

(30) Leofanti, G.; Padovan, M.; Tozzola, G.; Venturelli, B. Surface Area and Pore Texture of Catalysts. *Catal. Today* **1998**, *41* (1–3), 207–219. https://doi.org/10.1016/S0920-5861(98)00050-9.

(31) Alexandratos, S. D. Ion-Exchange Resins: A Retrospective from Industrial and Engineering Chemistry. *Ind. Eng. Chem. Res.* **2009**, *48*, 388–398. https://doi.org/10.1021/ie801242v.

(32) Badia i Córcoles, J. H. THESIS: Synthesis of Ethers as Oxygenated Additives for the Gasoline Pool, Universidad de Barcelona, **2016**.

(33) Smith, J. M. *Chemical Engineering Kinetics*, 3rd ed.; McGraw-Hill, Ed.; New York, **1981**.

(34) Wang, L.; Liu, X.; Wang, Y.; Sun, W.; Zhao, L. Thermodynamics and Reaction Kinetics of the Sorbitol Dehydration to Isosorbide Using NbOPO4 as the Catalyst. *Ind. Eng. Chem. Res.* **2022**. https://doi.org/10.1021/acs.iecr.2c00925.

APPENDIX

APPENDIX 1: HPLC Calibration

To determine the concentration of the substances, present in the mixture, it is necessary to calibrate the HPLC in order to know the relationship between the concentrations and the chromatographic areas of the compounds. For this purpose, standards of known composition are used to cover the range of possible concentrations present in the study. In addition, three analyses of each standard are performed to evaluate the statistical dispersion. Table 13 shows the calibration curves for sorbitol, isosorbide and sorbitans.

TABLE 13.Calibration curves for all the components of the SOH dehydration reaction system.

Component	Equation	R^2
SOH	$C_j = (1.87 \cdot 10^{-9} \pm 1.3 \cdot 10^{-10}) \cdot t + (3.19 \cdot 10^{-4} \pm 1.3 \cdot 10^{-3})$	0,994
IB	$C_j = (1.95 \cdot 10^{-9} \pm 1.1 \cdot 10^{-10}) \cdot t + (7.56 \cdot 10^{-4} \pm 5.2 \cdot 10^{-4})$	0,990
ST	$C_j = (1.81 \cdot 10^{-9} \pm 1 \cdot 10^{-10}) \cdot t + (7.48 \cdot 10^{-4} \pm 6{,}7 \cdot 10^{-4})$	0,995

It was decided to use the chromatographic areas and not the percent areas to obtain the calibration due to the formation of water after the two dehydrations. Since the HPLC mobile phase was water as well, it was impossible to analyze how much water was formed. That made it impossible to use the percent area. In addition, 2,5-sorbitan could not be found so the calibration of 1,4-sorbitan was used for this species since both are isomers.

APPENDIX 2: Cleaning of the experimental system

After the last sample was extracted, the stirring and heating system was stopped. The reactor was allowed to cool, the system was depressurized and the 3 safety screws were unscrewed. The reaction mixture was filtered to separate it from the catalyst and collected in two different vials. The reactor was cleaned with deionized water and dried. Next, the catalyst injection was checked for completeness. Then the internal accessories were cleaned. First, the solution residues are removed from the sampling circuit and then the reactor is cleaned with water. To do this, the reactor was filled with deionized water and the heating and stirring systems were turned on to flush out the remaining mixture. The water was pressurized and extracted through the sampling circuit. The extracted water was collected in an Erlenmeyer flask. Finally, the heating system was turned off to cool the reactor, the heating element was removed and the reactor was taken out. The reactor was cleaned with acetone and dried with synthetic air.

APPENDIX 3: Parity plots of the 56 kinetic models studied

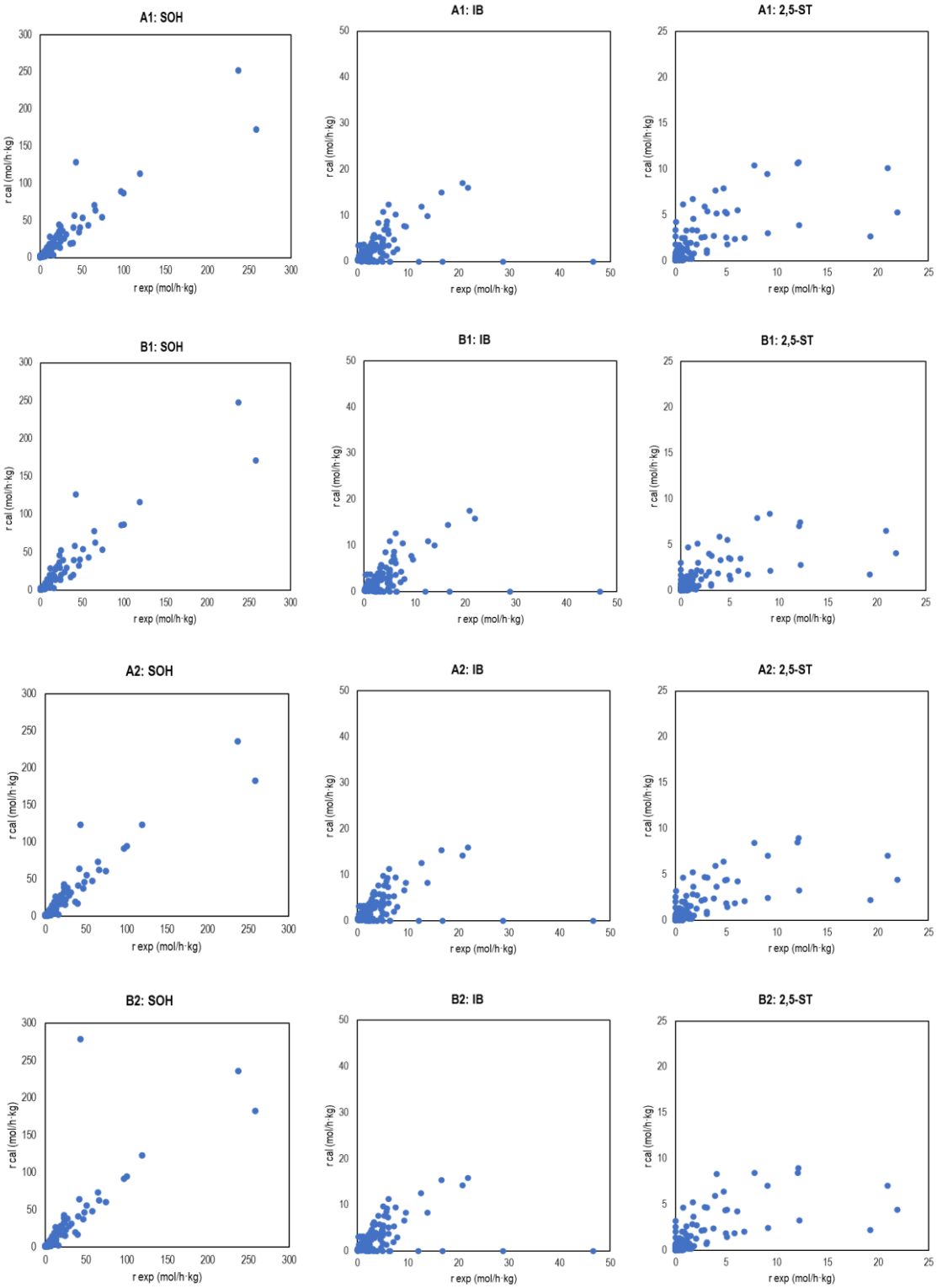

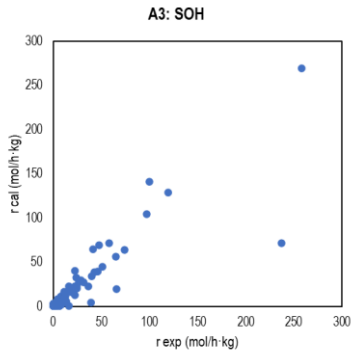
A3: SOH
r cal (mol/h·kg)
r exp (mol/h·kg)

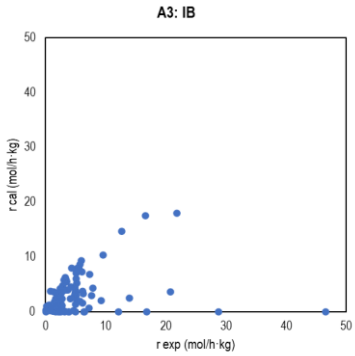
A3: IB
r cal (mol/h·kg)
r exp (mol/h·kg)

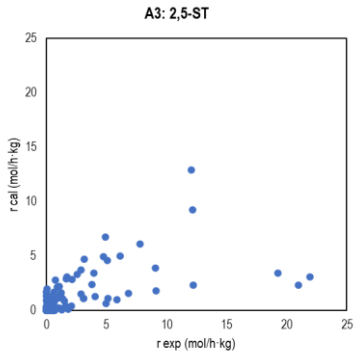
A3: 2,5-ST
r cal (mol/h·kg)
r exp (mol/h·kg)

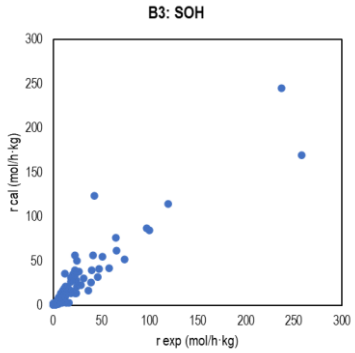
B3: SOH
r cal (mol/h·kg)
r exp (mol/h·kg)

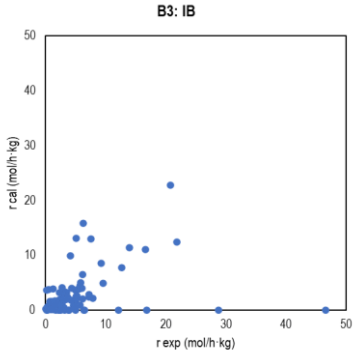
B3: IB
r cal (mol/h·kg)
r exp (mol/h·kg)

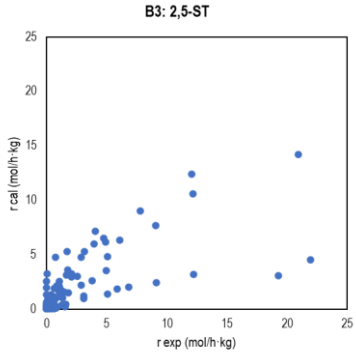
B3: 2,5-ST
r cal (mol/h·kg)
r exp (mol/h·kg)

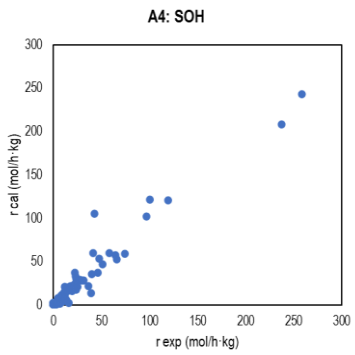
A4: SOH
r cal (mol/h·kg)
r exp (mol/h·kg)

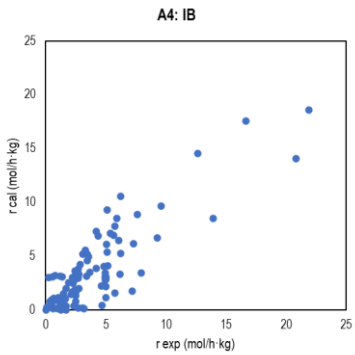
A4: IB
r cal (mol/h·kg)
r exp (mol/h·kg)

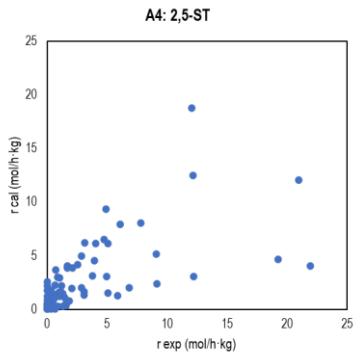
A4: 2,5-ST
r cal (mol/h·kg)
r exp (mol/h·kg)

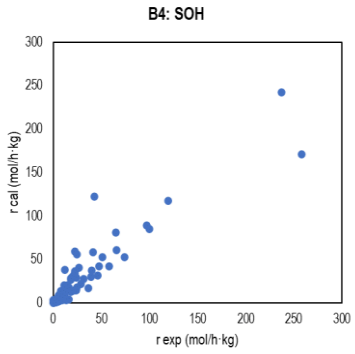
B4: SOH
r cal (mol/h·kg)
r exp (mol/h·kg)

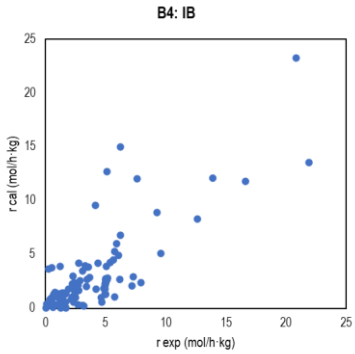
B4: IB
r cal (mol/h·kg)
r exp (mol/h·kg)

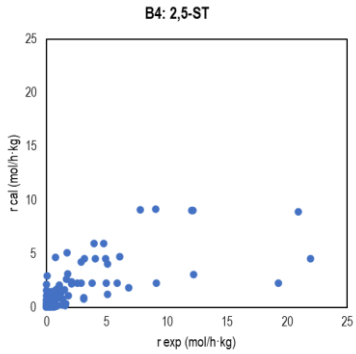
B4: 2,5-ST
r cal (mol/h·kg)
r exp (mol/h·kg)

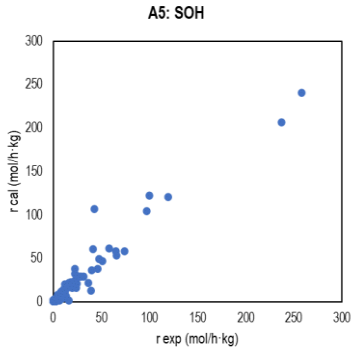
A5: SOH
r cal (mol/h·kg)
r exp (mol/h·kg)

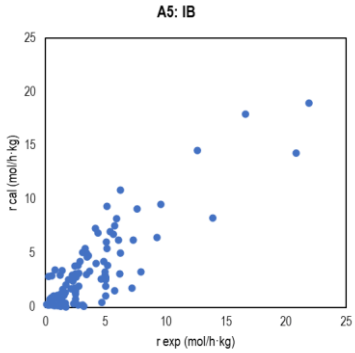
A5: IB
r cal (mol/h·kg)
r exp (mol/h·kg)

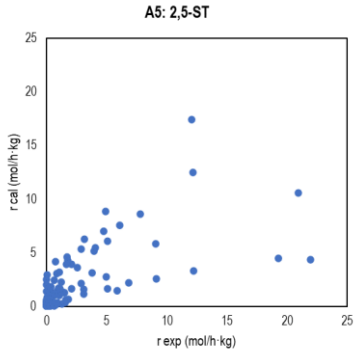
A5: 2,5-ST
r cal (mol/h·kg)
r exp (mol/h·kg)

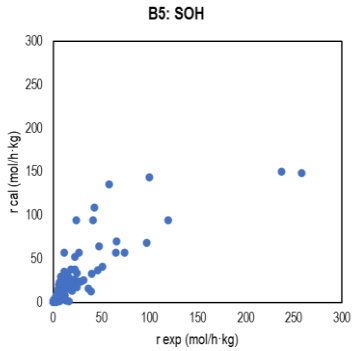
B5: SOH
r cal (mol/h·kg)
r exp (mol/h·kg)

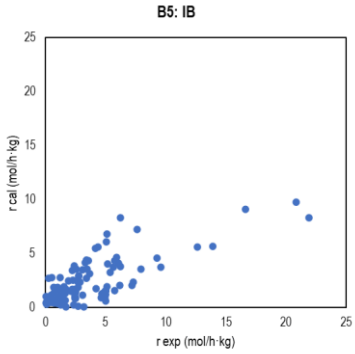
B5: IB
r cal (mol/h·kg)
r exp (mol/h·kg)

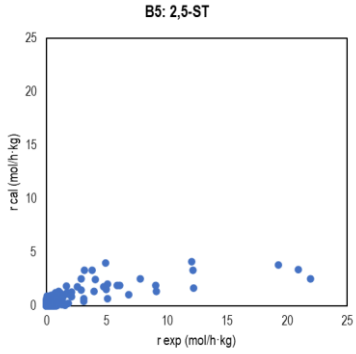
B5: 2,5-ST
r cal (mol/h·kg)
r exp (mol/h·kg)

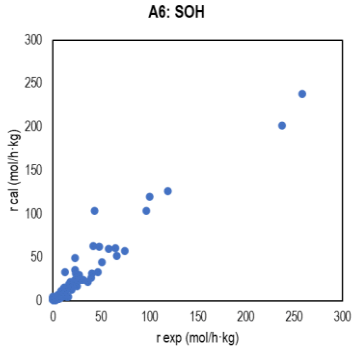
A6: SOH
r cal (mol/h·kg)
r exp (mol/h·kg)

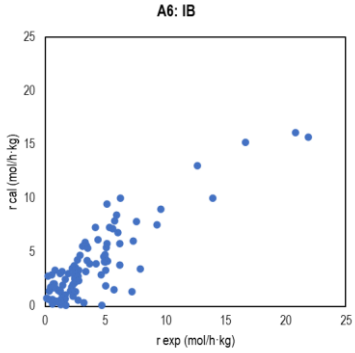
A6: IB
r cal (mol/h·kg)
r exp (mol/h·kg)

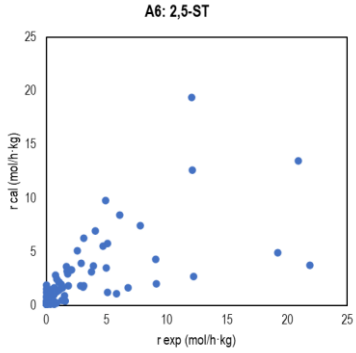
A6: 2,5-ST
r cal (mol/h·kg)
r exp (mol/h·kg)

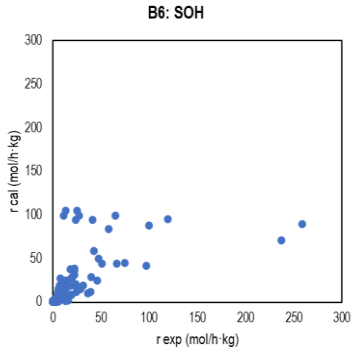
B6: SOH
r cal (mol/h·kg)
r exp (mol/h·kg)

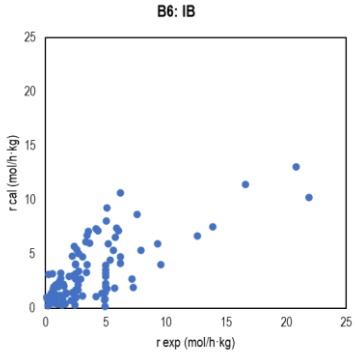
B6: IB
r cal (mol/h·kg)
r exp (mol/h·kg)

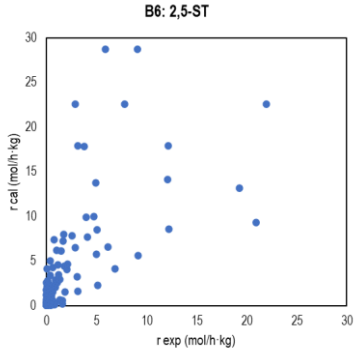
B6: 2,5-ST
r cal (mol/h·kg)
r exp (mol/h·kg)

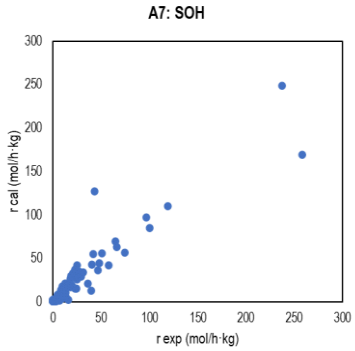
A7: SOH
r cal (mol/h·kg)
r exp (mol/h·kg)

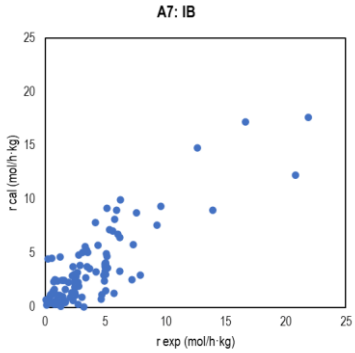
A7: IB
r cal (mol/h·kg)
r exp (mol/h·kg)

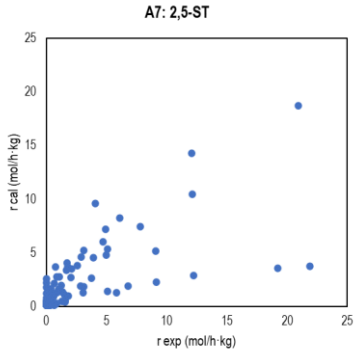
A7: 2,5-ST
r cal (mol/h·kg)
r exp (mol/h·kg)

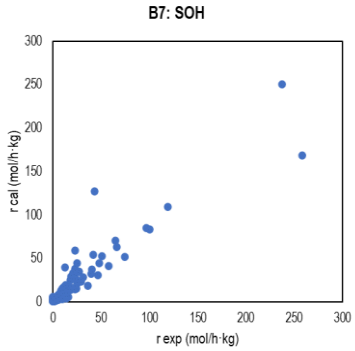
B7: SOH
r cal (mol/h·kg)
r exp (mol/h·kg)

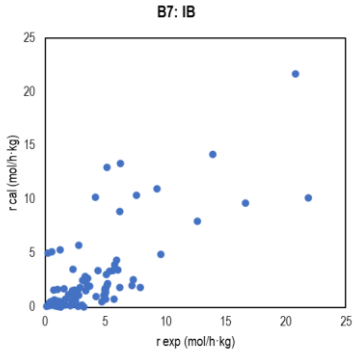
B7: IB
r cal (mol/h·kg)
r exp (mol/h·kg)

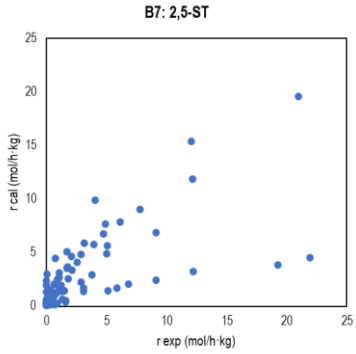
B7: 2,5-ST
r cal (mol/h·kg)
r exp (mol/h·kg)

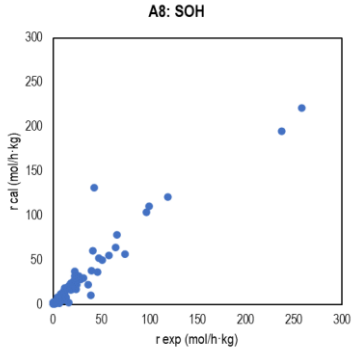
A8: SOH
r cal (mol/h·kg)
r exp (mol/h·kg)

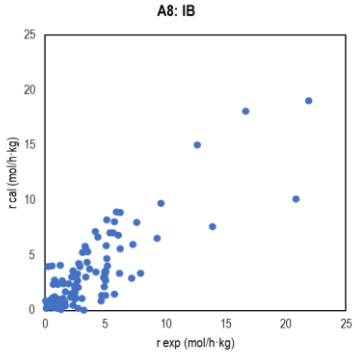
A8: IB
r cal (mol/h·kg)
r exp (mol/h·kg)

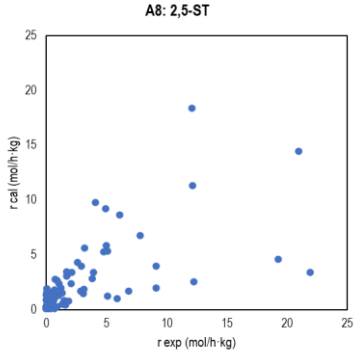
A8: 2,5-ST
r cal (mol/h·kg)
r exp (mol/h·kg)

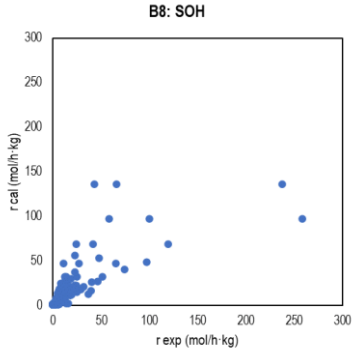
B8: SOH
r cal (mol/h·kg)
r exp (mol/h·kg)

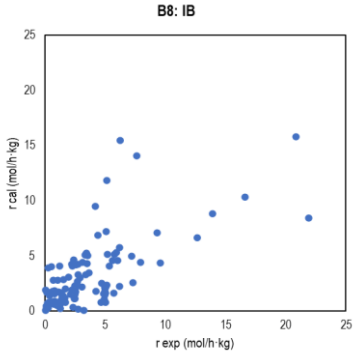
B8: IB
r cal (mol/h·kg)
r exp (mol/h·kg)

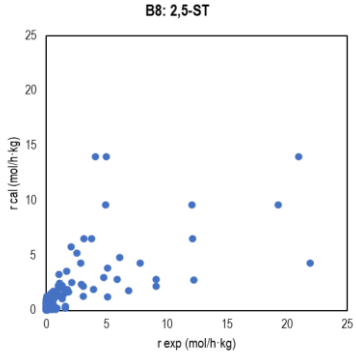
B8: 2,5-ST
r cal (mol/h·kg)
r exp (mol/h·kg)

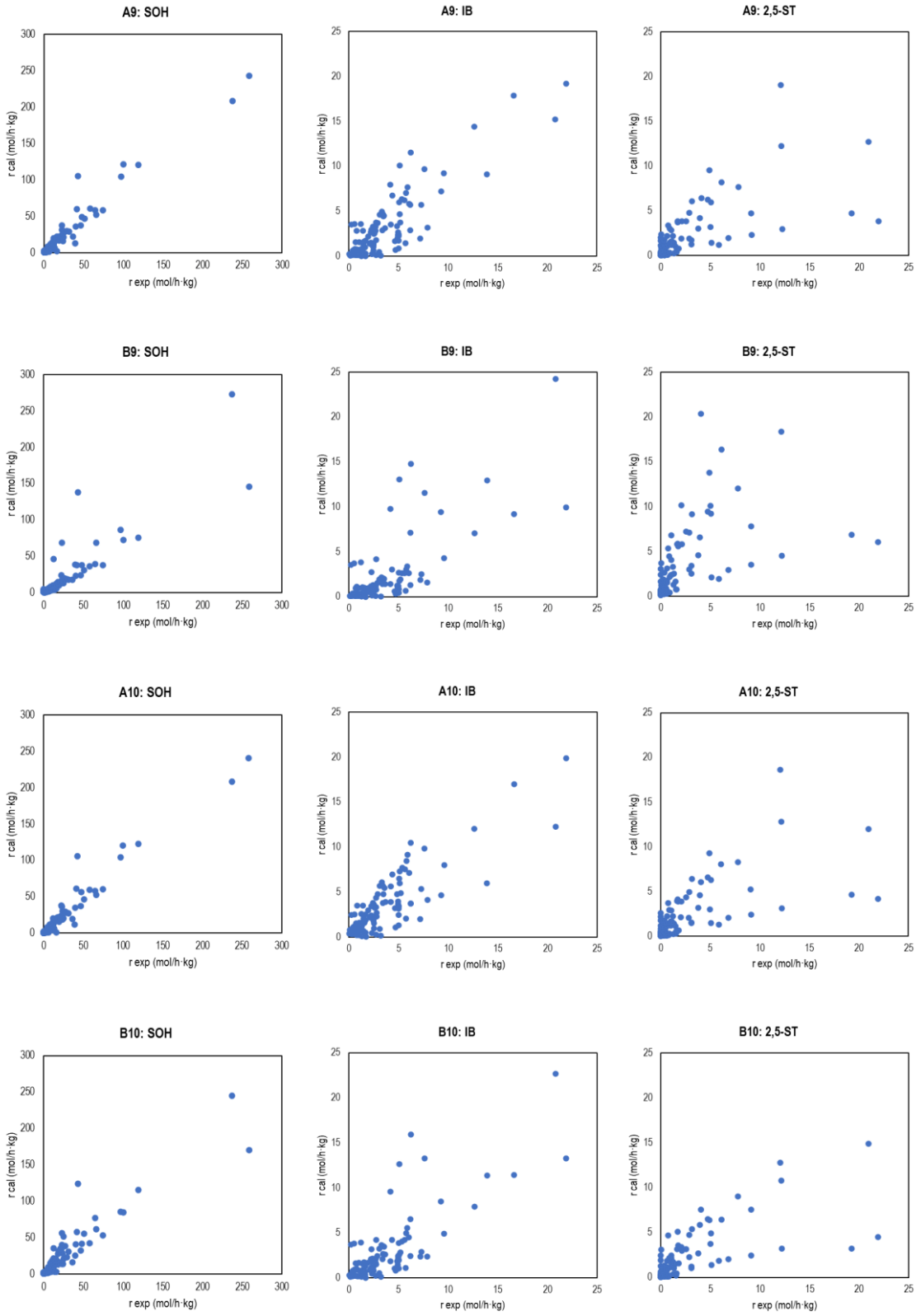
A9: SOH
A9: IB
A9: 2,5-ST
B9: SOH
B9: IB
B9: 2,5-ST
A10: SOH
A10: IB
A10: 2,5-ST
B10: SOH
B10: IB
B10: 2,5-ST
r cal (mol/h·kg)
r exp (mol/h·kg)

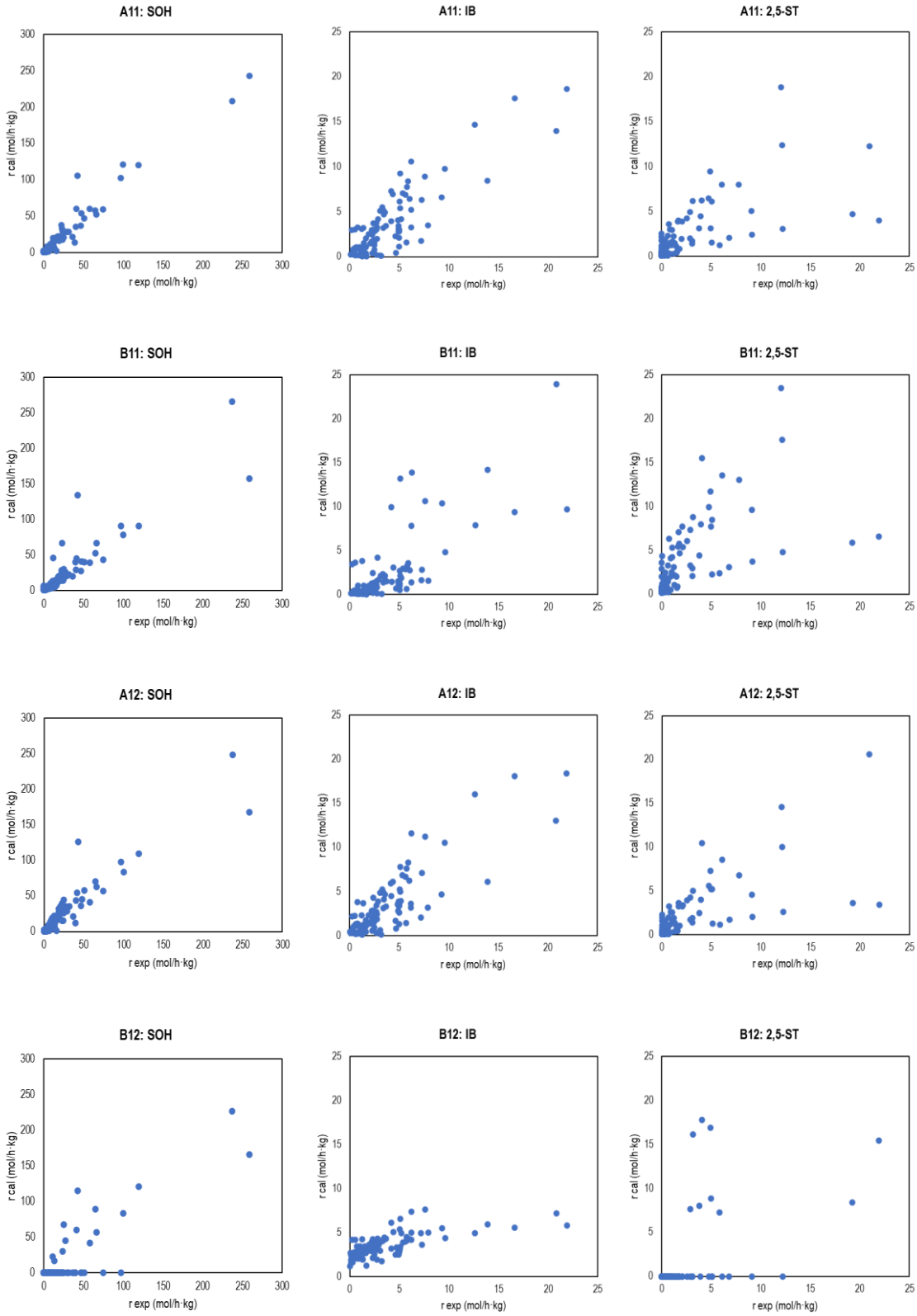
A11: SOH
A11: IB
A11: 2,5-ST
B11: SOH
B11: IB
B11: 2,5-ST
A12: SOH
A12: IB
A12: 2,5-ST
B12: SOH
B12: IB
B12: 2,5-ST
r cal (mol/h·kg)
r exp (mol/h·kg)

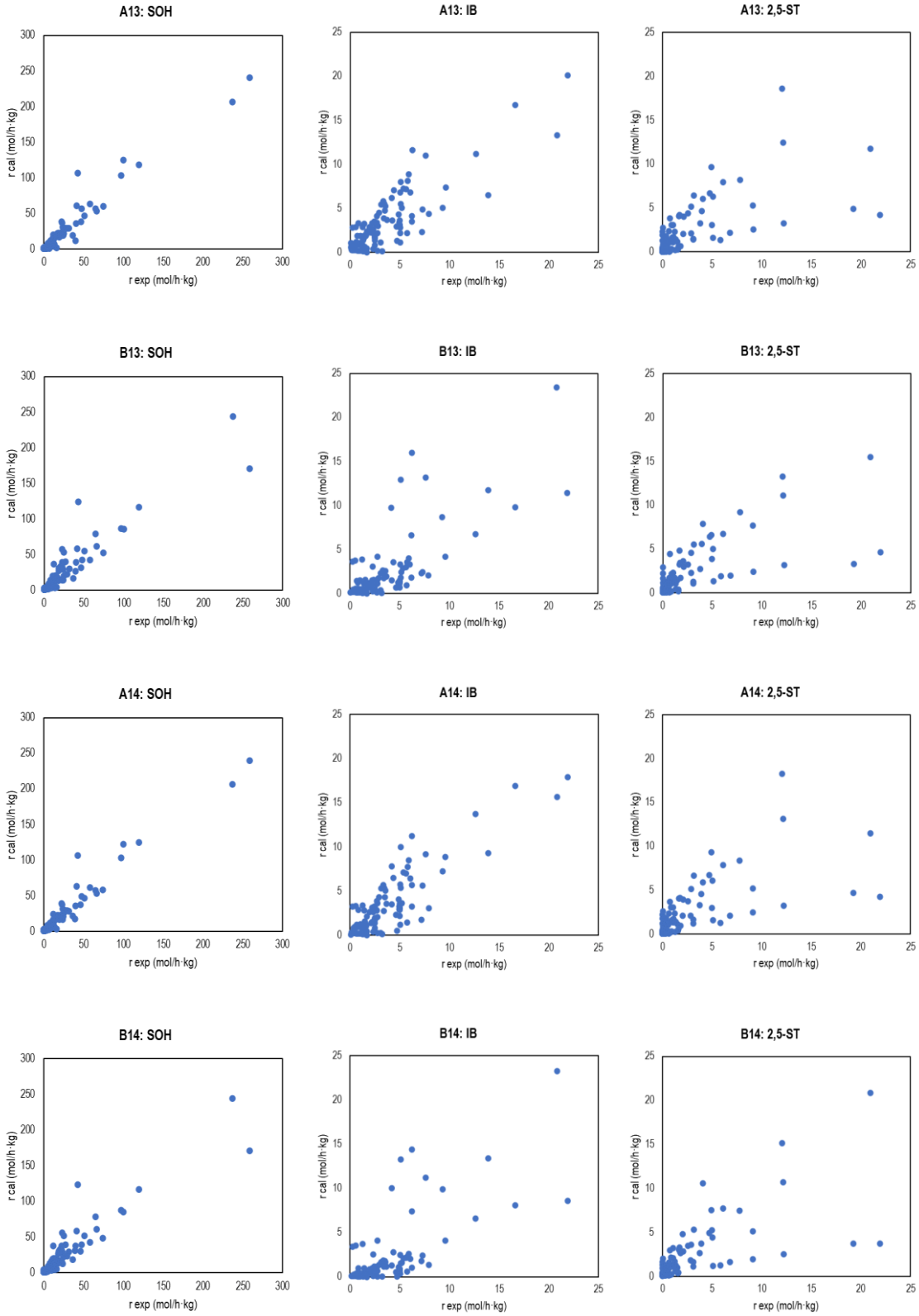
A13: SOH
A13: IB
A13: 2,5-ST
B13: SOH
B13: IB
B13: 2,5-ST
A14: SOH
A14: IB
A14: 2,5-ST
B14: SOH
B14: IB
B14: 2,5-ST
r cal (mol/h·kg)
r exp (mol/h·kg)

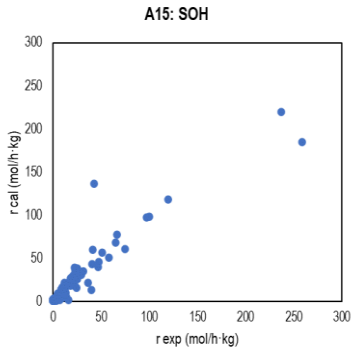
A15: SOH
r cal (mol/h·kg)
r exp (mol/h·kg)

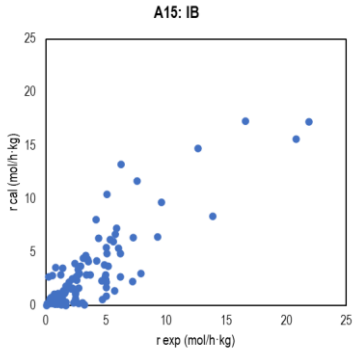
A15: IB
r cal (mol/h·kg)
r exp (mol/h·kg)

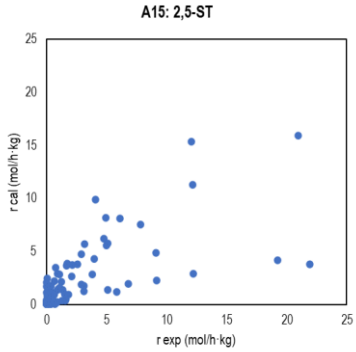
A15: 2,5-ST
r cal (mol/h·kg)
r exp (mol/h·kg)

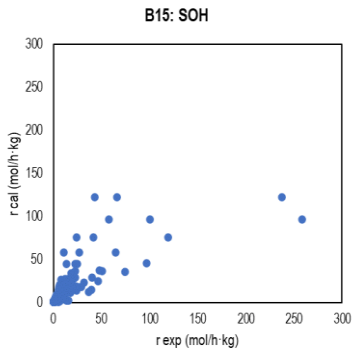
B15: SOH
r cal (mol/h·kg)
r exp (mol/h·kg)

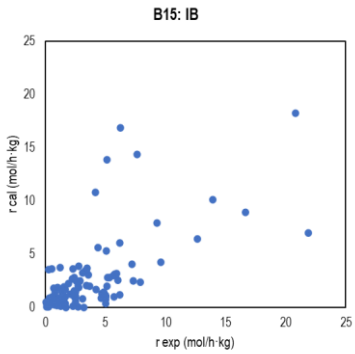
B15: IB
r cal (mol/h·kg)
r exp (mol/h·kg)

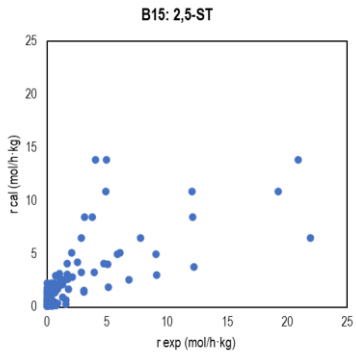
B15: 2,5-ST
r cal (mol/h·kg)
r exp (mol/h·kg)

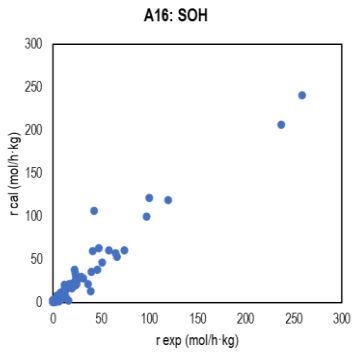
A16: SOH
r cal (mol/h·kg)
r exp (mol/h·kg)

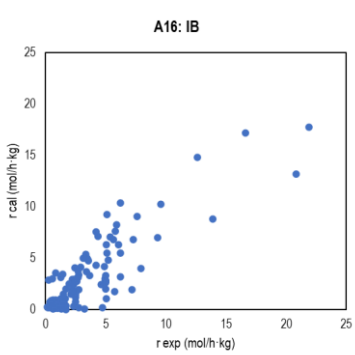
A16: IB
r cal (mol/h·kg)
r exp (mol/h·kg)

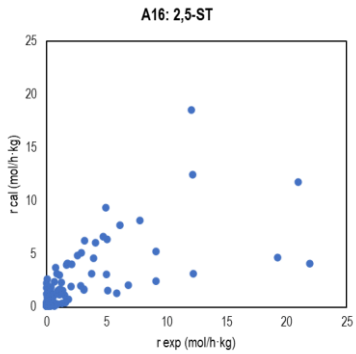
A16: 2,5-ST
r cal (mol/h·kg)
r exp (mol/h·kg)

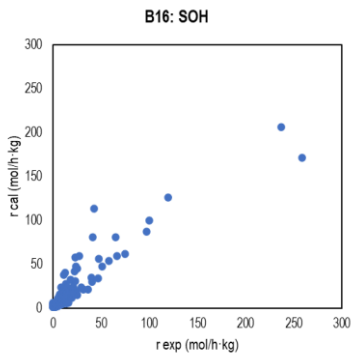
B16: SOH
r cal (mol/h·kg)
r exp (mol/h·kg)

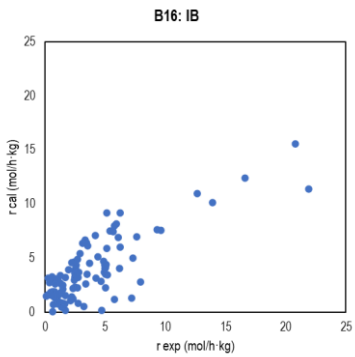
B16: IB
r cal (mol/h·kg)
r exp (mol/h·kg)

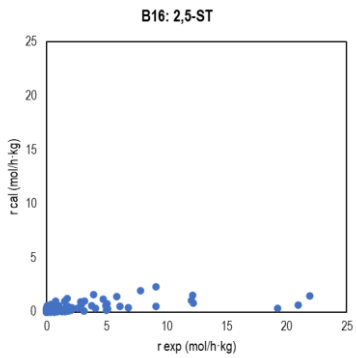
B16: 2,5-ST
r cal (mol/h·kg)
r exp (mol/h·kg)

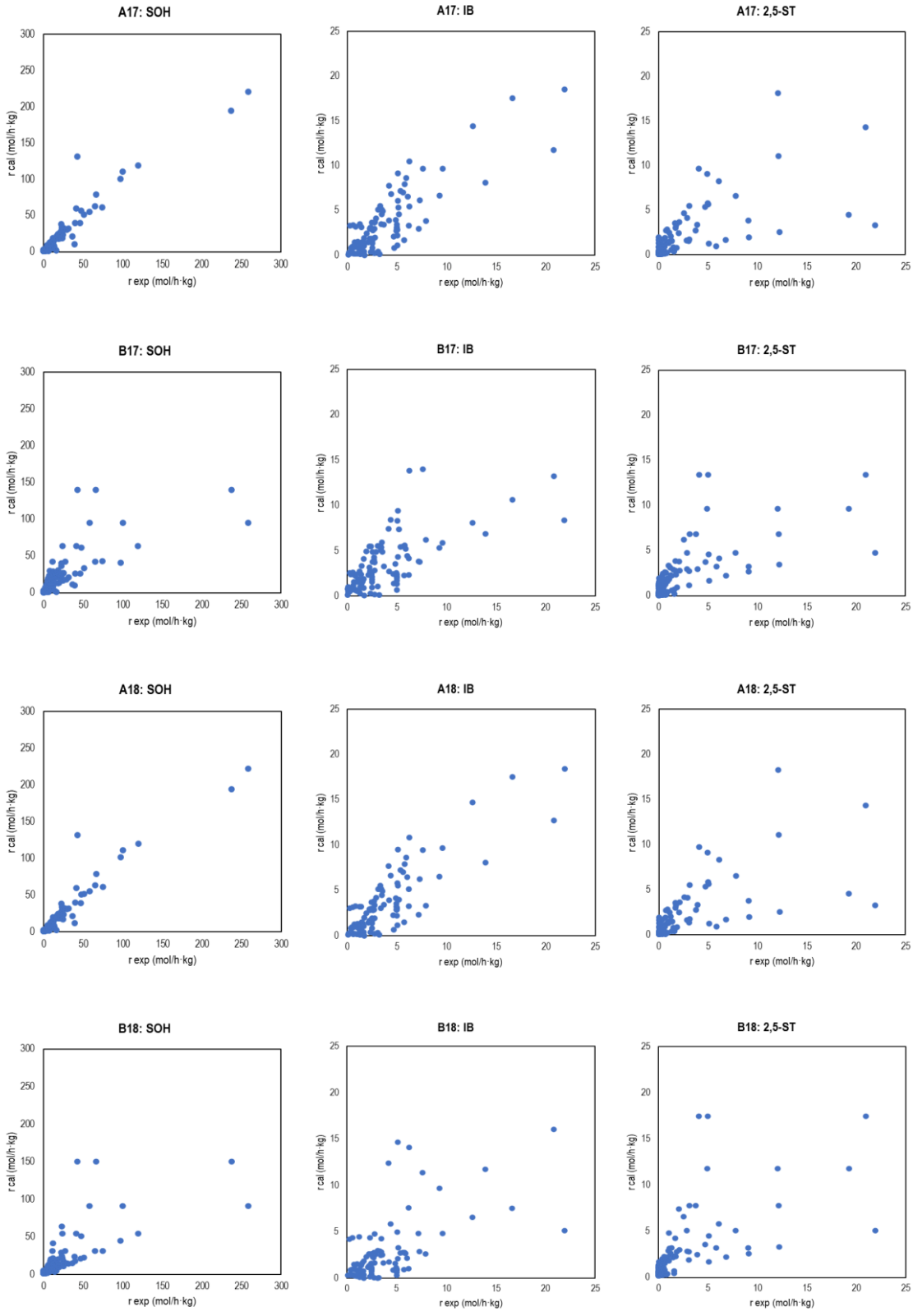
A17: SOH
A17: IB
A17: 2,5-ST
B17: SOH
B17: IB
B17: 2,5-ST
A18: SOH
A18: IB
A18: 2,5-ST
B18: SOH
B18: IB
B18: 2,5-ST
r cal (mol/h·kg)
r exp (mol/h·kg)

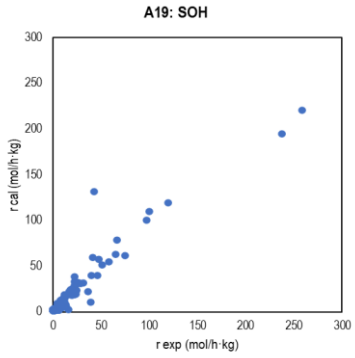
A19: SOH
r cal (mol/h·kg)
r exp (mol/h·kg)

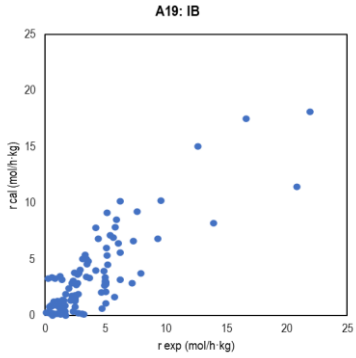
A19: IB
r cal (mol/h·kg)
r exp (mol/h·kg)

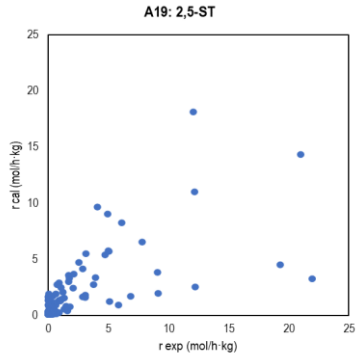
A19: 2,5-ST
r cal (mol/h·kg)
r exp (mol/h·kg)

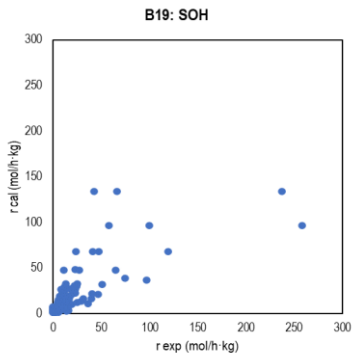
B19: SOH
r cal (mol/h·kg)
r exp (mol/h·kg)

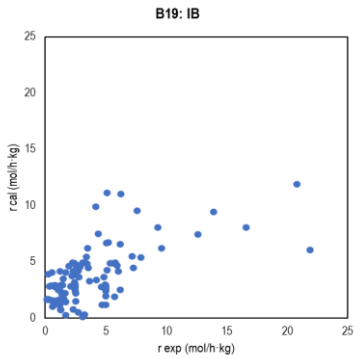
B19: IB
r cal (mol/h·kg)
r exp (mol/h·kg)

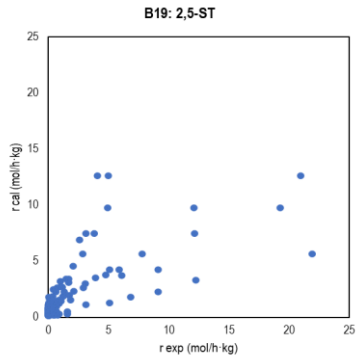
B19: 2,5-ST
r cal (mol/h·kg)
r exp (mol/h·kg)

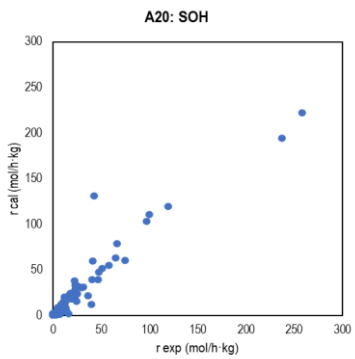
A20: SOH
r cal (mol/h·kg)
r exp (mol/h·kg)

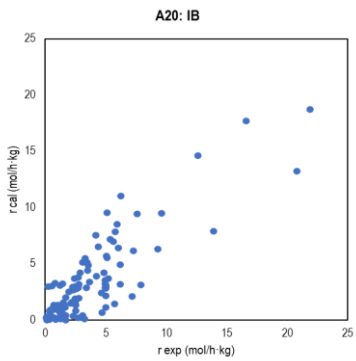
A20: IB
r cal (mol/h·kg)
r exp (mol/h·kg)

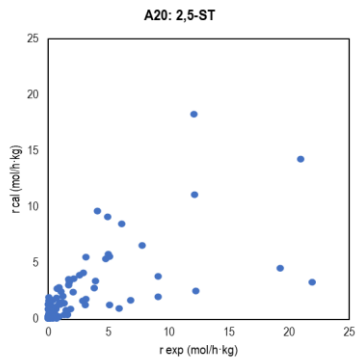
A20: 2,5-ST
r cal (mol/h·kg)
r exp (mol/h·kg)

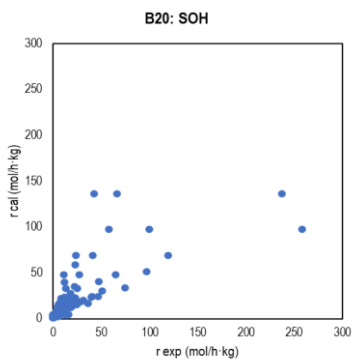
B20: SOH
r cal (mol/h·kg)
r exp (mol/h·kg)

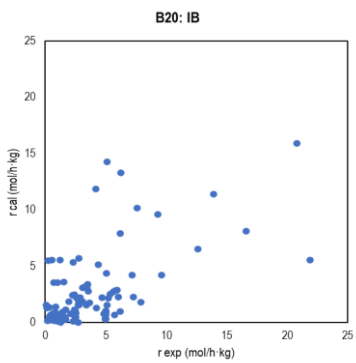
B20: IB
r cal (mol/h·kg)
r exp (mol/h·kg)

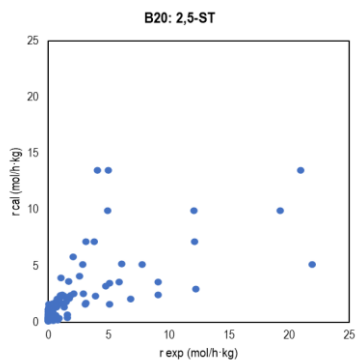
B20: 2,5-ST
r cal (mol/h·kg)
r exp (mol/h·kg)

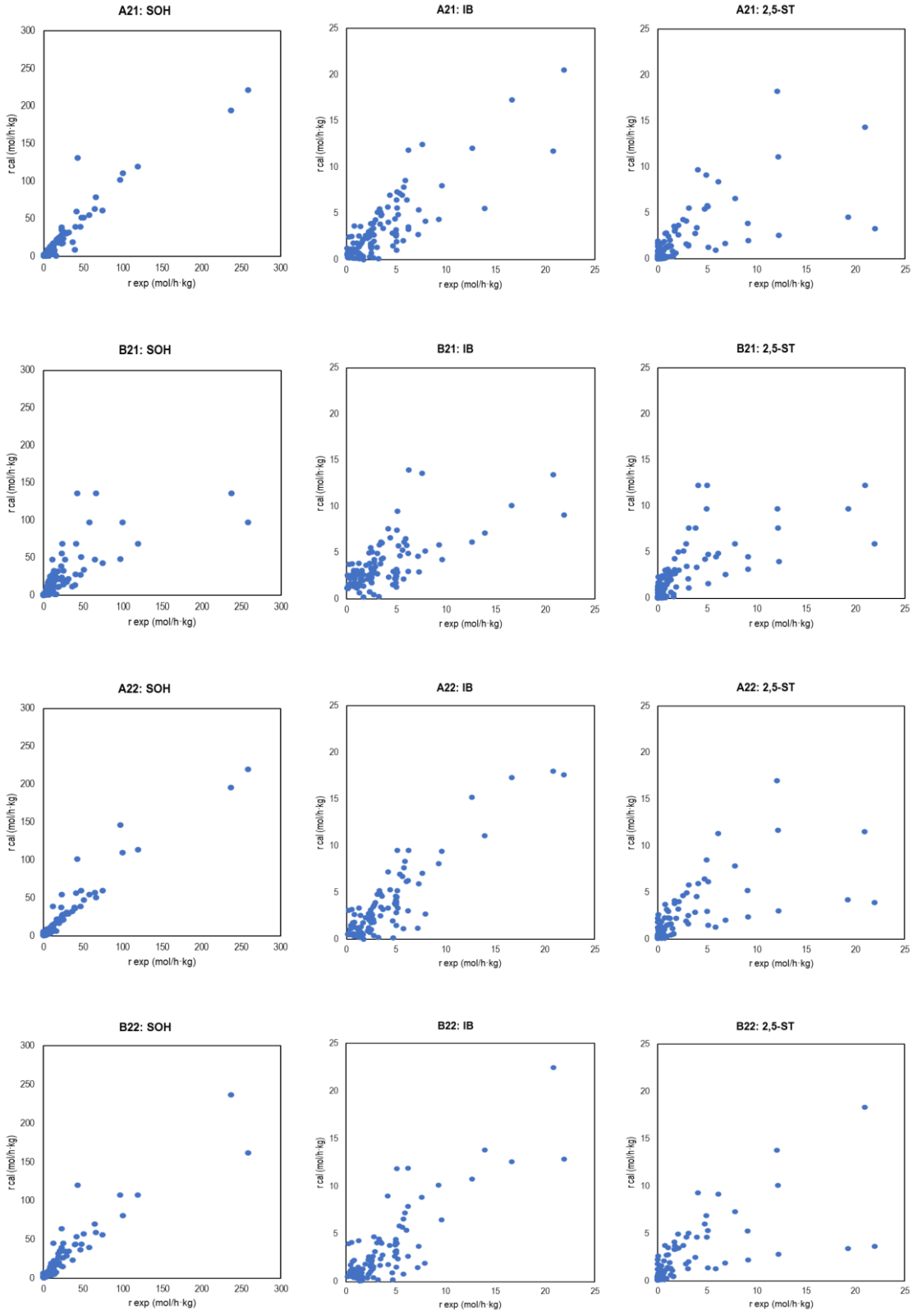
A21: SOH
A21: IB
A21: 2,5-ST
B21: SOH
B21: IB
B21: 2,5-ST
A22: SOH
A22: IB
A22: 2,5-ST
B22: SOH
B22: IB
B22: 2,5-ST
r cal (mol/h·kg)
r exp (mol/h·kg)

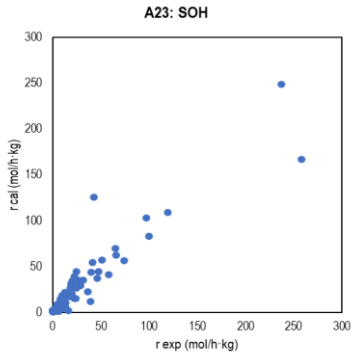
A23: SOH
r cal (mol/h·kg)
r exp (mol/h·kg)

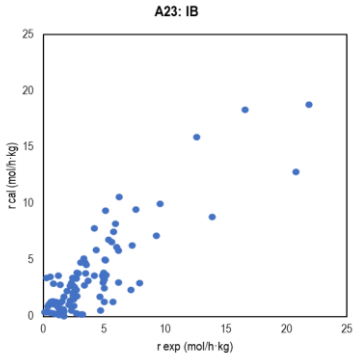
A23: IB
r cal (mol/h·kg)
r exp (mol/h·kg)

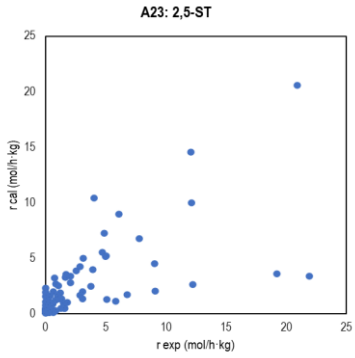
A23: 2,5-ST
r cal (mol/h·kg)
r exp (mol/h·kg)

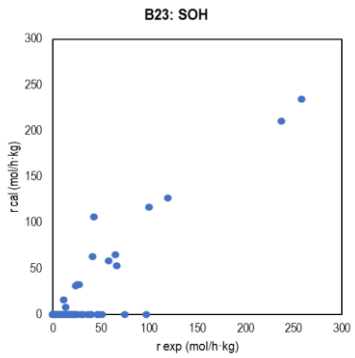
B23: SOH
r cal (mol/h·kg)
r exp (mol/h·kg)

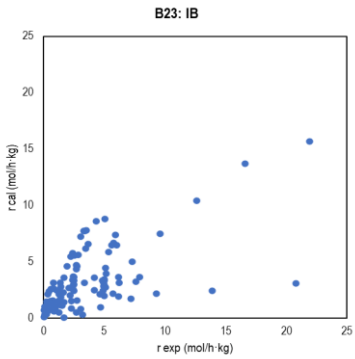
B23: IB
r cal (mol/h·kg)
r exp (mol/h·kg)

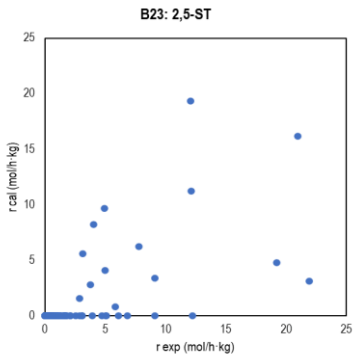
B23: 2,5-ST
r cal (mol/h·kg)
r exp (mol/h·kg)

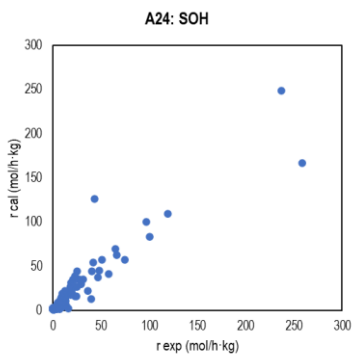
A24: SOH
r cal (mol/h·kg)
r exp (mol/h·kg)

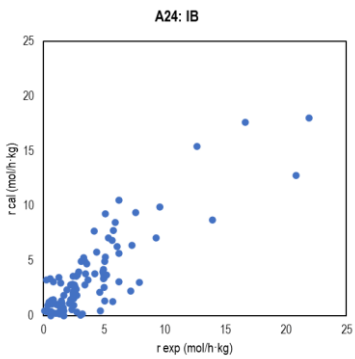
A24: IB
r cal (mol/h·kg)
r exp (mol/h·kg)

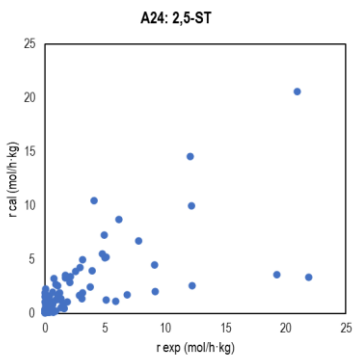
A24: 2,5-ST
r cal (mol/h·kg)
r exp (mol/h·kg)

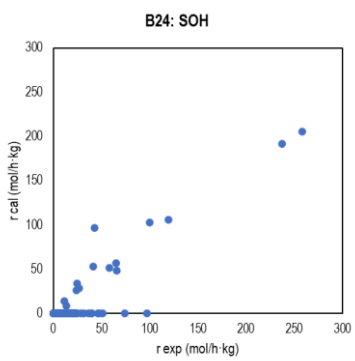
B24: SOH
r cal (mol/h·kg)
r exp (mol/h·kg)

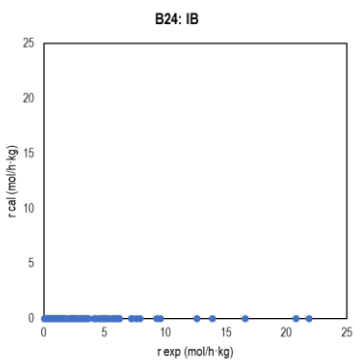
B24: IB
r cal (mol/h·kg)
r exp (mol/h·kg)

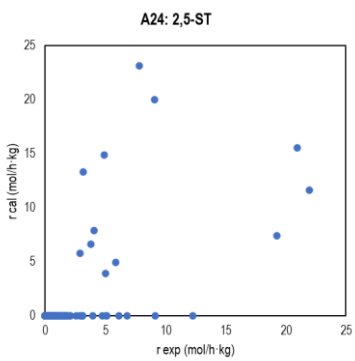
A24: 2,5-ST
r cal (mol/h·kg)
r exp (mol/h·kg)

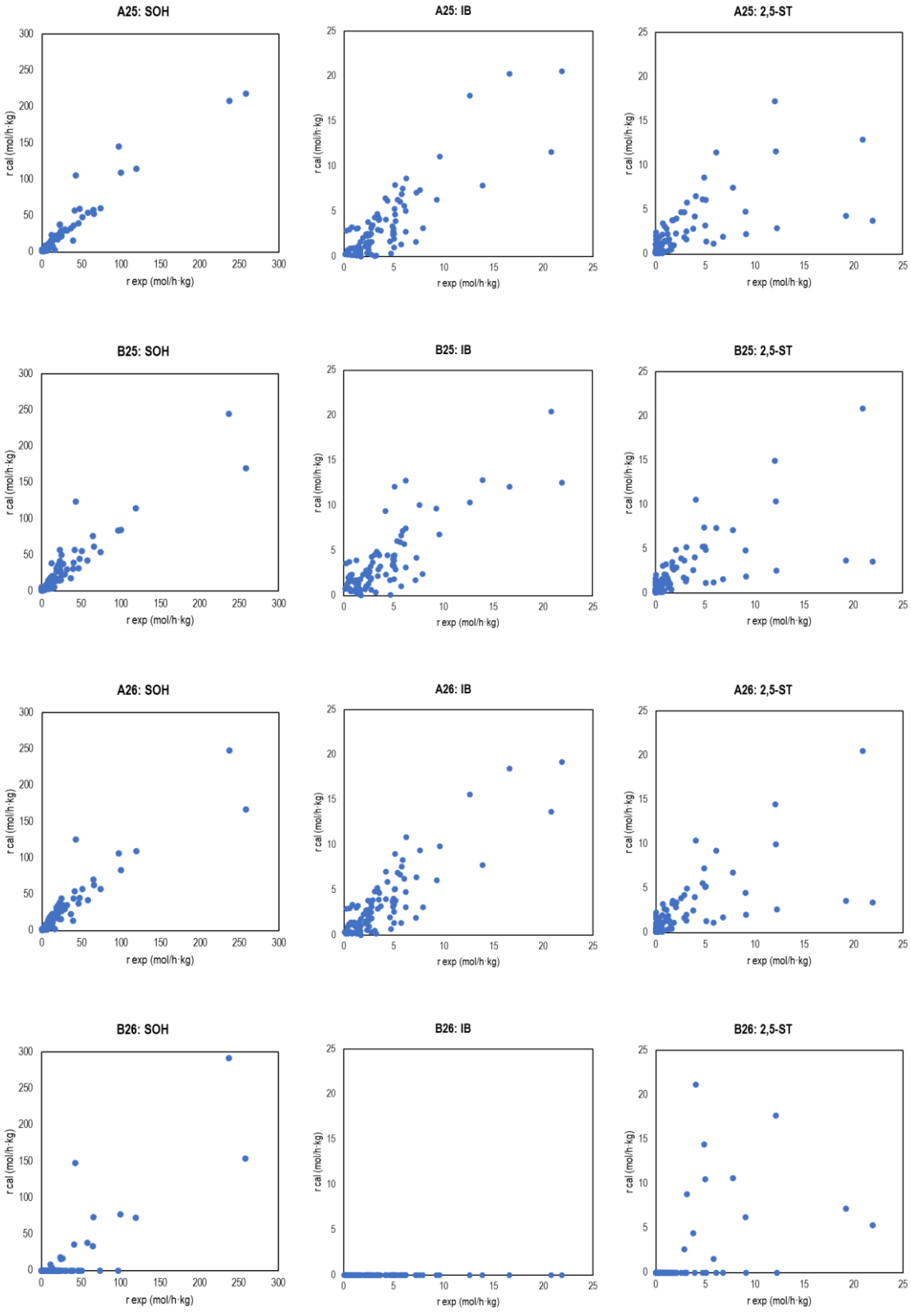
A25: SOH
A25: IB
A25: 2,5-ST
B25: SOH
B25: IB
B25: 2,5-ST
A26: SOH
A26: IB
A26: 2,5-ST
B26: SOH
B26: IB
B26: 2,5-ST
r cal (mol/h·kg)
r exp (mol/h·kg)

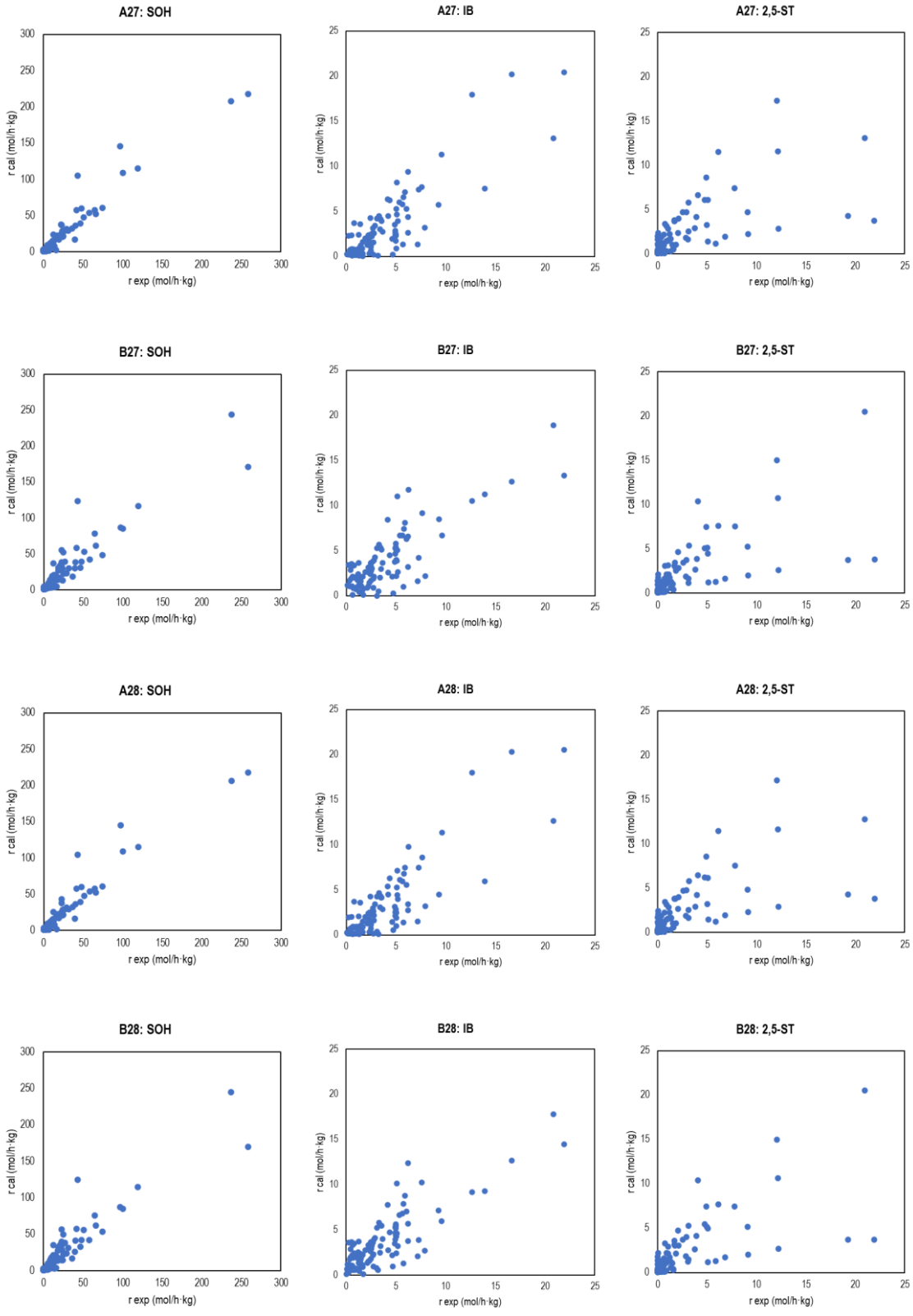
A27: SOH
A27: IB
A27: 2,5-ST
B27: SOH
B27: IB
B27: 2,5-ST
A28: SOH
A28: IB
A28: 2,5-ST
B28: SOH
B28: IB
B28: 2,5-ST
r cal (mol/h·kg)
r exp (mol/h·kg)